Bioorganic Chemistry 112 (2021) 104879

Contents lists available at ScienceDirect

Bioorganic Chemistry

journal homepage: www.elsevier.com/locate/bioorg

Design, synthesis and evaluation of cinnamic acid hybrids as multi-target-directed agents for the treatment of Alzheimer's disease

Keren Wang [a,1], Jian Shi [a,1], Yi Zhou [a], Ying He [a], Jing Mi [a], Jing Yang [a], Shuang Liu [a], Xiangcheng Tang [a], Wenmin Liu [a], Zhenghuai Tan [b,*], Zhipei Sang [a,*]

[a] College of Chemistry and Pharmaceutical Engineering, Nanyang Normal University, Nanyang 473061, China
[b] Institute of Traditional Chinese Medicine Pharmacology and Toxicology, Sichuan Academy of Chinese Medicine Sciences, Chengdu 610041, China

ARTICLE INFO

Keywords:
Alzheimer's disease
Cinnamic acid hybrids
Multi-function agents
$AlCl_3$-induced zebrafish
Scopolamine-induced memory impairment
Stability study

ABSTRACT

Herein, combining 1,2,3,4-tetrahydroisoquinoline and benzylpiperidine groups into cinnamic acid derivatives, a series of novel cinnamic acid hybrids was rationally designed, synthesized and evaluated by the multi-target-directed ligands (MTDLs) strategy. Hybrid **4e** was the most promising one among these hybrids with a reversible *hu*BuChE inhibitor (IC_{50} = 2.5 μM) and good MAO-B inhibition activity (IC_{50} = 1.3 μM) and antioxidant potency (ORAC = 0.4 eq). Moreover, compound **4e** significantly inhibited self-mediated $A\beta_{1\text{-}42}$ aggregation (65.2% inhibition rate). Compound **4e** exhibited remarkable anti-inflammatory propery and neuroprotective effect. Furthermore, compound **4e** displayed favourable blood–brain barrier penetration *via* parallel artificial membrane permeation assay (PAMPA). The obtained results also revealed that compound **4e** significantly improved dyskinesia recovery rate and response efficiency on AD model zebrafish. Further, **4e** did not show obvious acute toxicity at dose up to 1500 mg/kg *in vivo* and improved scopolamine-induced memory impairment. Importantly, compound **4e** showed good stability in both artificial gastric fluid and artificial intestinal fluid. Therefore, compound **4e** presented a promising multi-targeted active molecule for treating AD.

1. Introduction

Alzheimer's disease (AD), one of the greatest public health challenges, is a neurodegenerative brain disease, characterized by chronic progressive cognitive impairment and behavioral abnormalities. It is estimated by the 2019 report of Alzheimer Disease International that dementia afflicting>50 million people worldwide and the figure of the AD patients will triple by 2050 [1].

In spite of enormous efforts have been made, the exact etiological cause of AD still unknown. While molecular pathogeneses share common some abnormal changes in the brain of AD patients, including low levels of acetylcholine (ACh), amyloid-β (Aβ) deposits, hyperphosphorylated tau neurofibrillary tangles, biometal ion dyshomeostasis, and elevated oxidative stress [2,3]. To date, clinical FDA-approved anti-AD drugs mainly concentrate on acetylcholinesterase (AChE) inhibitors, for instance, rivastigmine, donepezil, and galantamine. These drugs restore cognitive functions and alleviate symptoms of AD by enhancing the level of ACh [4]. Long-term clinical applications show that effective of the AChE inhibitors is temporary and limited [5,6]. Furthermore, the AD patients suffer from serious side effects (nausea, diarrhea and vomiting) after taking the AChE inhibitors [7,8]. Hence, the explore for new drugs remains desirable.

Given the intricate nature of AD, controlling the single-target cannot be effective. MTDLs that can simultaneously interact with multiple AD-associated targets has been adopted as a more effective treatment strategy [9–12].

The cholinergic hypothesis posits that AD is correlated to loss of cholinergic function in the central nervous system. Accumulation of evidences show that the levels of AChE increase only in the early to moderate stage. While the AChE levels slightly reduce and the BuChE levels increase to 165% of the normal level in late stage, implying that BuChE takes over the role of AChE in the late stage of AD [13–15]. Therefore, targeting BuChE has been a useful way to treat the advanced AD [16].

The abnormal aggregation of the Aβ triggers complex pathological cascade leading to neurodegeneration, reckons the Aβ cascade

* Corresponding authors.
E-mail addresses: tanzhh616@163.com (Z. Tan), sangzhipei@126.com (Z. Sang).
[1] These authors contributed equally.

https://doi.org/10.1016/j.bioorg.2021.104879
Received 12 February 2021; Received in revised form 1 March 2021; Accepted 26 March 2021
Available online 9 April 2021
0045-2068/© 2021 Elsevier Inc. All rights reserved.

hypothesis, a dominant hypothesis of AD [17]. The increased Aβ prone to aggregate into soluble oligomers, which triggers neuroinflammation, neurofibrillary tangles and neuronal death, leading to AD [18,19]. Thus, inhibiting accumulation of Aβ has great potential for AD treatment.

Increasing researches reveal that MAO-B increases dramatically in the AD brain and contributes to produce hydroxyl radicals, which accelerates Aβ aggregations [20]. What's more, the launched selective MAO-B inhibitor, Selegiline, shows the improvement for both cognition and activities of daily living in a clinical trial in people with mild-to-moderate AD [21]. In conclusion, the design of compounds that can inhibit the activity of MAO-B is of value in the treatment of AD.

Cinnamic acid (3-phenylprop-2-enoic acid) and its simple derivatives (p-coumaric acid and ferulic acid) are widely presented in plants. These derivatives possess potent antioxidant, anti-inflammatory and neuroprotective properties [22–24]. All of these advantages indicate Cinnamic acid and its simple derivatives is a potential lead compounds for the treatment of neurodegenerative diseases, such as AD and Parking disease. While the low bioavailability limits their clinical use [25–29]. In addition, selectively inhibiting BuChE serves as a potent approach for addressing AD, and both the 1,2,3,4-tetrahydroisoquinoline and benzylpiperidine groups have been verified to be beneficial for the selective BuChE inhibitory activities based on our previous work [30–32]. Therefore, we plan to fuse the 1,2,3,4-tetrahydroisoquinoline and benzylpiperidine groups into cinnamic acid derivatives by MTDLs to obtain a series of cinnamic acid hybrids (Fig. 1). The synthesized compounds are assessed by ChEs inhibition, MAOs inhibition, antioxidant activity, inhibition of Aβ aggregation, neuroprotective effects, effects on $AlCl_3$-induced zebrafish AD and scopolamine-induced memory impairment.

2. Results and discussion

2.1. Chemistry

The synthetic route of cinnamic acid hybrids **4a-4q** and **5a ~ 5p** was outlined in Scheme 1. Organic acid (**1a ~ 1r**) were reacted with 1,2,3,4-tetrahydroisoquinoline and benzylpiperidine, respectively, in the presence of 1-ethyl-3-(3-dimethylaminopropyl)carbodiimide hydrochloride (EDCI) and 1-Hydroxybenzotriazole (HOBt) in CH_2Cl_2 at room temperature to obtain the cinnamic acid hybrids, yield from 52%~88%. Finally, the target structures were confirmed by ^{1}H NMR, ^{13}C NMR and HR-ESI-MS spectroscopy.

2.2. Biological activity

2.2.1. Inhibition of AChE and BuChE

All the synthesized target derivatives were evaluated for their inhibitory potency against *ee*AChE (from *electrophorus electricus*) and *eq*BuChE (from *equine serum*) *via* the Ellman's method [31–33]. Donepezil was taken as the positive control. Further, the target compounds with good inhibitory activity against *ee*AChE or *eq*BuChE were

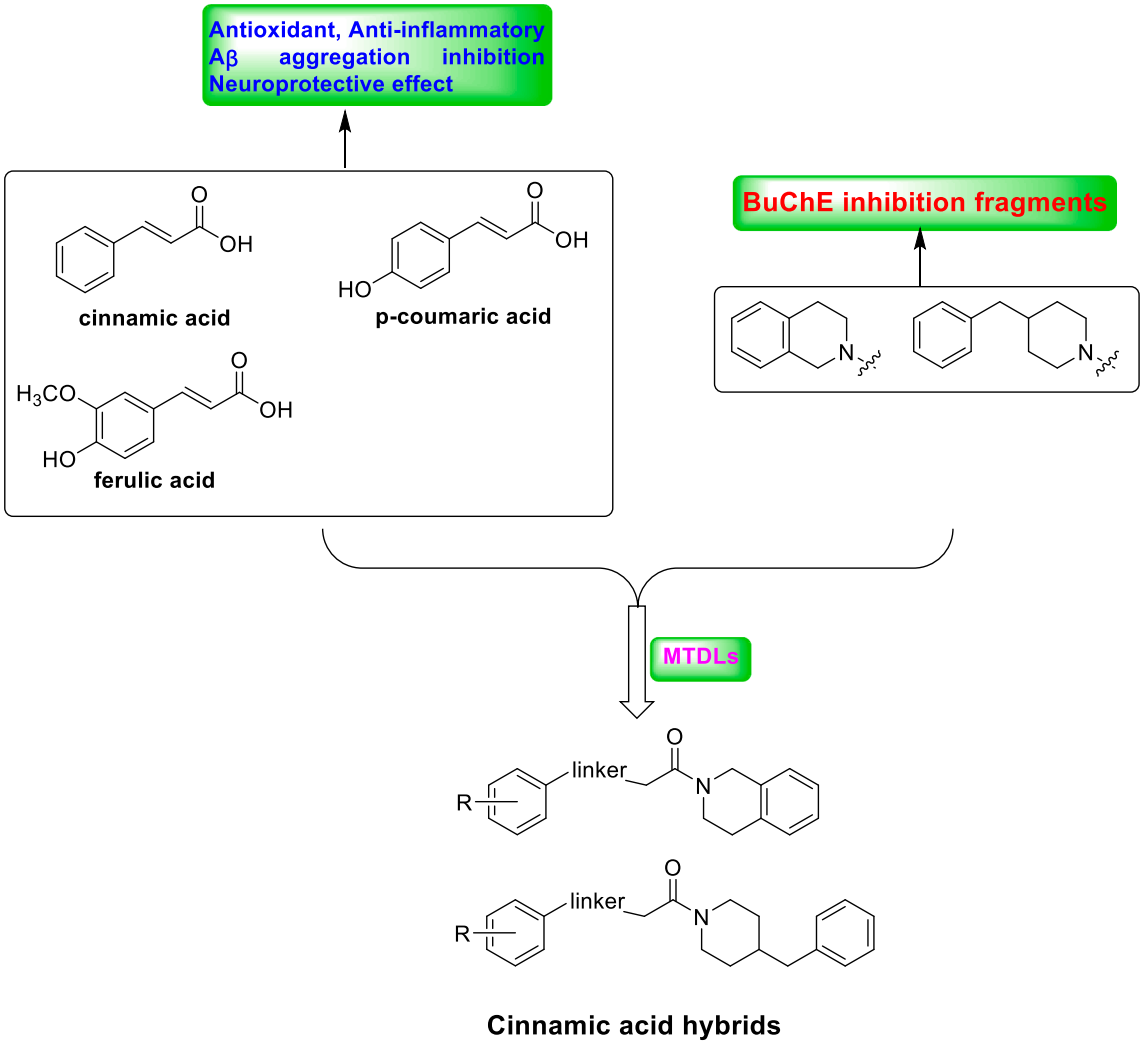

Fig. 1. Design strategy of cinnamic acid hybrids.

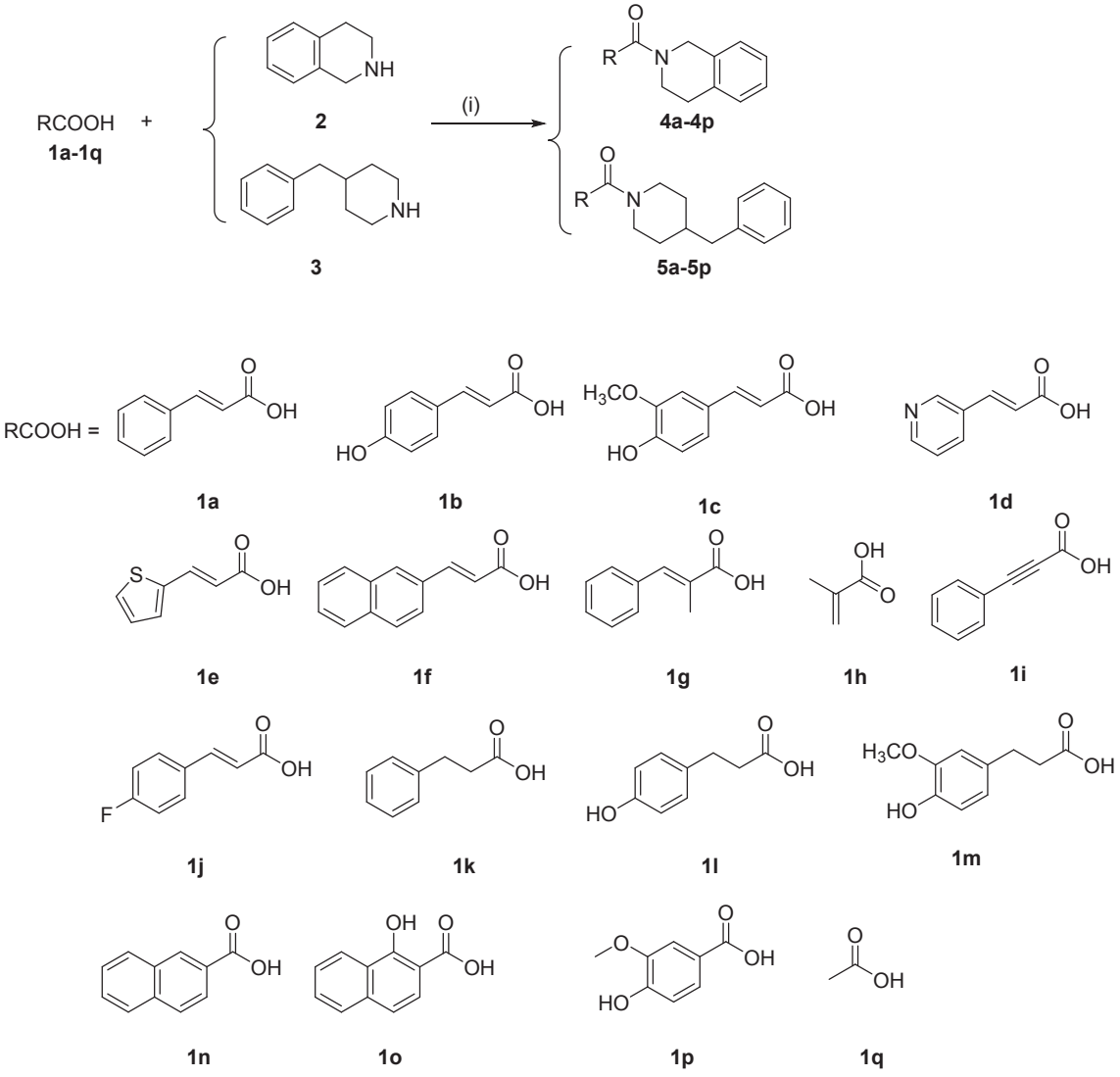

Scheme 1. Synthesis of cinnamic acid hybrids (**4a** ~ **4p** and **5a** ~ **5p**). Reagents and conditions: (i) CH_2Cl_2, EDCI, HOBt, room temperature, overnight.

reconfirmed by *hu*AChE (human AChE) or *hu*BuChE (human BuChE). Table 1 displayed all the cinnamic acid hybrids **4a** ~ **4p** and **5a** ~ **5p** displayed weak *ee*AChE inhibitory activity, displaying that both the orgainc acid skeleton and the secondary amine fragments did not produce significant effect on *ee*AChE inhibitory activity. According to the screening data, some of these derivatives showed good *eq*BuChE inhibitory potency, both the orgainc acid skeleton and the secondary amine fragments remarkably influenced the BuChE inhibitory potency. When the secondary amine was 1,2,3,4-tetrahydroisoquinoline, target compounds **4b**, **4c** and **4e** exhibited good *eq*BuChE inhibitory actvity, which were better BuChE inhibitory activity than other derivatives. The structure–activity-relationship (SAR) indicated that compound **4a** with cinnamic acid skeleton showed potential *eq*BuChE inhibitory activity (IC_{50} = 6.1 μM), when the benzene ring of cinnamic acid in **4a** was substituted by hydroxy group to get compounds **4b** and **4c**, respectively, the *eq*BuChE inhibitory potency significantly increased to 3.9 and 4.1 μM, respectively. While the benzene ring was substituted with F atom to obtain compound **4j**, the inhibitory potency decreased to 39.8 μM. Then when the the benzene ring of **4a** was replaced with pyridine and naphthalene to get compounds **4d** and **4f**, respectively, the *eq*BuChE inhibitory activity declined to > 50 and 11.5 μM, respectively, while the benzene ring of **4a** was replaced with thiophene to get compound **4e,** the *eq*BuChE inhibitory potency increased to 2.1 μM. Moreover, when the cinnamic acid of **4a** was replaced with (*E*)-2-methyl-3-phenylacrylic acid and 3-phenylpropiolic acid to get compounds **4 g** and **4i**, respectively, the *eq*BuChE inhibitory potency slightly decreased to 12.6 and 8.8 μM, respectively, revealing that the olefin contributed to the *eq*BuChE inhibitory activity. When the cinnamic acid of **4a** was replaced with methacrylic acid to get **4 h**, the inhibitory potency slightly declined to 9.5 μM. Furthermore, when the olefin group of compounds **4a**, **4b** and **4c** were reduced to get compounds **4 k**, **4 l** and **4 m**, respectively, the *eq*BuChE inhibitory potency significantly decreased to 30.3, 30.2 and 10.9 μM, respectively. Further, when removing the olefin fragment, we got compounds **4n** (IC_{50} = 18.3 μM), **4o** (IC_{50} = 14.1 μM) and **4p** (IC_{50} = 10.6 μM), which showed moderate *eq*BuChE inhibitory potency. Similarly, when the secondary amine was benzylpiperidine, compounds **5 g**, **5 h** an **5 l** showed the best *eq*BuChE inhibitory activity with IC_{50} values of 3.7, 3.3 and 4.3 μM, respectively. The SAR displayed that compound **5a** with cinnamic acid fragment displayed moderate *eq*BuChE inhibitory activity (IC_{50} value = 15.2 μM). When the cinnamic acid fragment was replaced with *p*-coumaric acid, (*E*)-3-(thiophen-2-yl)acrylic acid, (*E*)-3-(naphthalen-2-yl)acrylic acid, (*E*)-2-methyl-3-phenylacrylic acid and (*E*)-3-(4-fluorophenyl)acrylic acid to get compounds **5b** (IC_{50} = > 50 μM), **5d** (IC_{50} = 32.7 μM), **5e** (IC_{50} = 11.5 μM), **5f** (IC_{50} = 13.2 μM)and **5i** (IC_{50} = 34.7 μM), the inhibitory activity did not present obvious changes. While when the cinnamic acid fragment of **5a** was replaced

Table 1
In vitro IC_{50} values of test compounds toward the AChE/BuChE.

Compounds	RCOOH	IC_{50} ± SD (μM)[a] *Ee*AChE	*Eq*BuChE	SI[b]	IC_{50} ± SD (μM)[a] *hu*AChE	*hu*BuChE
4a	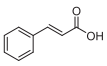	15.9 ± 1.3	6.1 ± 0.2	2.6	*n.t.*[c]	*n.t.*[c]
4b	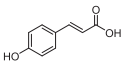	17.4 ± 1.2	3.9 ± 0.4	4.5	*n.t.*[c]	6.3 ± 0.08
4c	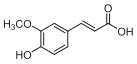	30.5 ± 1.3	4.1 ± 0.5	1.9	*n.t.*[c]	*n.t.*[c]
4d	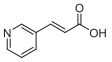	38.9 ± 1.2	> 50	—	*n.t.*[c]	*n.t.*[c]
4e	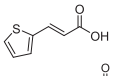	19.4 ± 1.5	2.1 ± 0.08	9.2	*n.t.*[c]	2.5 ± 0.09
4f	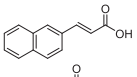	15.7 ± 1.1	11.5 ± 0.8	1.4	*n.t.*[c]	*n.t.*[c]
4 g	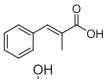	26.9 ± 1.6	12.6 ± 1.1	2.1	*n.t.*[c]	*n.t.*[c]
4 h		30.4 ± 2.6	9.5 ± 0.6	3.2	*n.t.*[c]	*n.t.*[c]
4i		25.8 ± 1.7	8.8 ± 0.4	2.9	*n.t.*[c]	*n.t.*[c]
4j	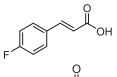	16.9 ± 1.3	39.8 ± 2.6	0.4	*n.t.*[c]	*n.t.*[c]
4 k	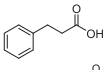	17.5 ± 1.4	30.3 ± 2.8	0.6	*n.t.*[c]	*n.t.*[c]
4 l	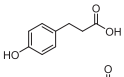	17.3 ± 1.9	30.2 ± 2.7	0.6	*n.t.*[c]	*n.t.*[c]
4 *m*	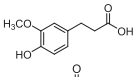	15.4 ± 0.8	10.9 ± 0.7	1.4	*n.t.*[c]	*n.t.*[c]
4*n*	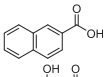	25.9 ± 2.2	18.3 ± 0.9	1.4	*n.t.*[c]	*n.t.*[c]
4o	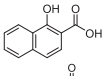	16.1 ± 0.9	14.1 ± 1.3	1.1	*n.t.*[c]	*n.t.*[c]
4p	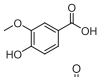	17.2 ± 1.3	10.6 ± 0.8	1.6	*n.t.*[c]	*n.t.*[c]
5a	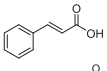	16.4 ± 1.5	15.2 ± 1.8	1.1	*n.t.*[c]	*n.t.*[c]
5b	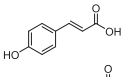	13.8 ± 1.6	> 50	—	*n.t.*[c]	*n.t.*[c]
5c	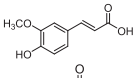	26.2 ± 2.1	7.2 ± 1.1	3.6	*n.t.*[c]	*n.t.*[c]
5d	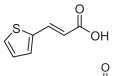	27.8 ± 2.4	32.7 ± 2.9	0.9	*n.t.*[c]	*n.t.*[c]
5e	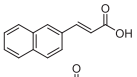	15.7 ± 1.1	11.5 ± 0.9	1.4	*n.t.*[c]	*n.t.*[c]
5f	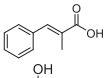	22.7 ± 1.3	13.2 ± 1.1	1.7	*n.t.*[c]	*n.t.*[c]
5 g		26.6 ± 1.7	3.7 ± 0.3	9.9	*n.t.*[c]	6.6 ± 0.7
5 h		16.5 ± 1.2	3.3 ± 0.2	5	*n.t.*[c]	5.9 ± 0.4
5i	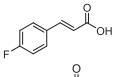	19.5 ± 1.4	34.7 ± 3.1	0.6	*n.t.*[c]	*n.t.*[c]
5j	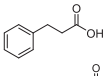	16.5 ± 1.1	33.6 ± 2.9	0.5	*n.t.*[c]	*n.t.*[c]
5 k	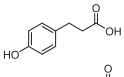	15.7 ± 1.5	16.5 ± 1.9	1	*n.t.*[c]	*n.t.*[c]
5 l	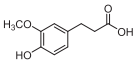	21.3 ± 2.2	4.3 ± 0.7	5	*n.t.*[c]	7.6 ± 0.5

(*continued on next page*)

Table 1 (*continued*)

Compounds	RCOOH	IC_{50} ± SD (μM)[a] *Ee*AChE	*Eq*BuChE	SI[b]	IC_{50} ± SD (μM)[a] *hu*AChE	*hu*BuChE
5 *m*	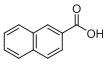	27.1 ± 1.4	14.6 ± 1.3	1.9	*n.t.*[c]	*n.t.*[c]
5*n*	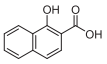	13.9 ± 1.8	10.4 ± 1.1	1.3	*n.t.*[c]	*n.t.*[c]
5o	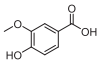	21.8 ± 1.8	29.5 ± 2.1	0.7	*n.t.*[c]	*n.t.*[c]
5p	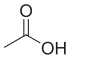	30.7 ± 2.6	30.4 ± 1.9	1	*n.t.*[c]	*n.t.*[c]
donepezil		0.015 ± 0.0005	5.1 ± 0.04	0.003	0.012 ± 0.0003	6.4 ± 0.26

[a] the experiments were performed by three time and expressed as means ± SD. [b] SI = Selectivity Index = IC_{50} (*ee*AChE)/IC_{50} (*eq*BuChE). [c] n.t. = not tested.

with were ferulic acid, methacrylic acid and 3-phenylpropiolic acid to get compounds **5c**, **5 g** and **5 h**, respectively, the *eq*BuChE inhibitory activity significantly increased to 7.2, 3.7 and 3.3 μM. In addition, when the olefin group were reduced, we obtained compounds **5j**, **5 k** and **5 l**, compounds **5j** and **5 k** showed weak *eq*BuChE inhibitory activity, while compound **5 l** showed good *eq*BuChE inhibitory activity (IC_{50} = 4.3 μM). Furthermore, when removing the olefin group, we got compounds **5 m**, **5n**, **5o** and **5p**, exhibiting weak *eq*BuChE inhibitory activity with IC_{50} values of 14.6, 10.4, 29.5 and 30.4 μM. Therefore, based on the above data, compounds **4b**, **4e**, **5 g**, **5 h** an **5 l** were re-tested using *hu*BuChE, the data in Table 1 displayed potent *hu*BuChE inhibitory potency with IC_{50} values of 6.3, 2.5, 6.6, 5.9 and 7.6 μM, which were worth in-depth study.

2.2.2. *The reversibility study of huBuChE inhibition by **4e***

To determine the reversibility of *hu*BuChE inhibition by target derivatives, the best BuChE inhibitor **4e** was selected to test the recovery of *hu*BuChE inhibition [33]. As shown in Fig. 2**A**, in comparison to controls, *hu*BuChE activity decreased to 3.6% by the 0.1 × IC_{50} of standard rivastigmine , while increased to 11.8% by the 0.1 × IC_{50} of donepezil. Meanwhile, 0.1 × IC_{50} compound **4e** increased *hu*BuChE activity to 9.3%. This suggests that huBuChE may not be able to recover from

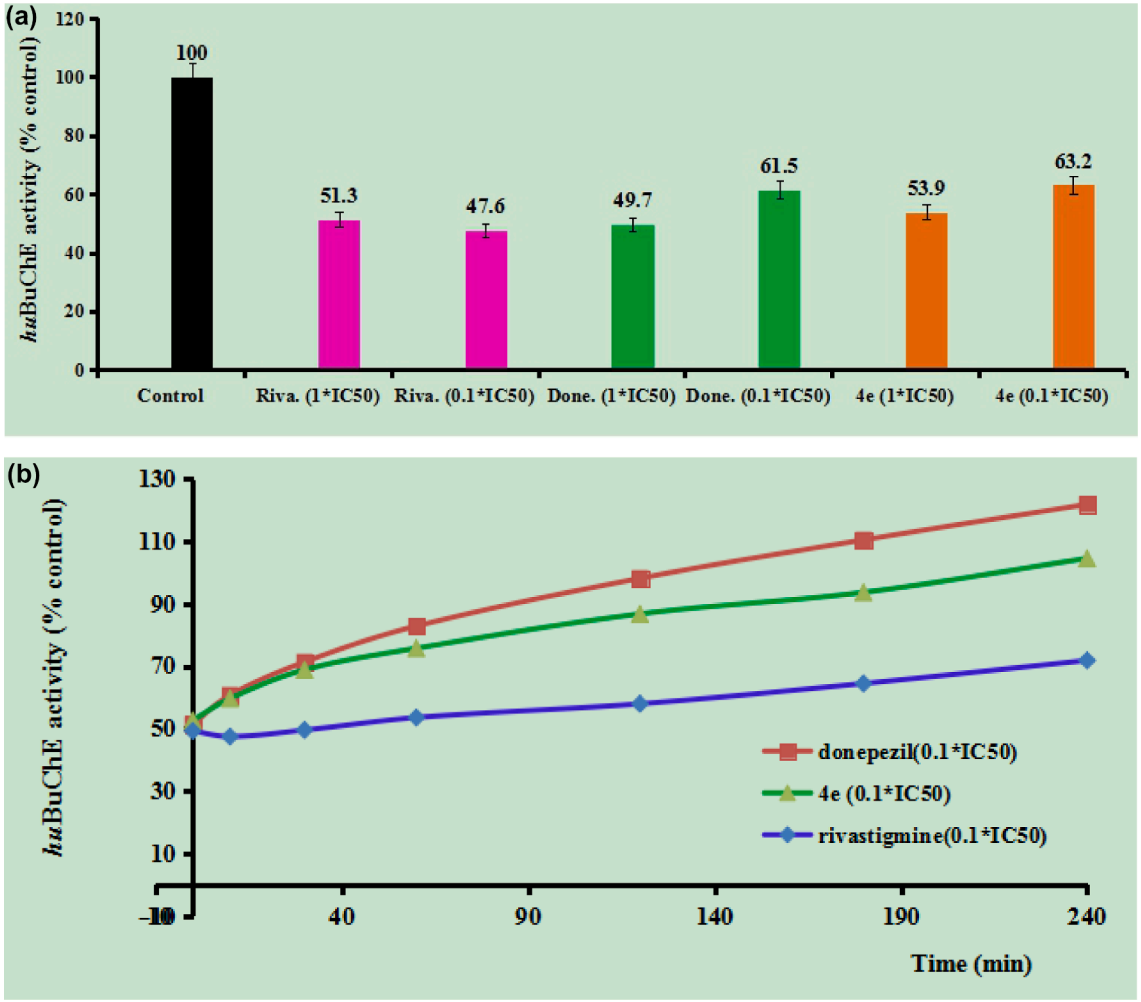

Fig. 2. (A) The *hu*BuChE reversibility of inhibition by **4e** after diluting to 0.1 × IC_{50} by contrast with donepezil and rivastigmine. (B) The *hu*BuChE reversibility of donepezil, rivastigmine, and **4e** was monitored with time after dilution to 0.1 × IC_{50}.

rivastigmine inhibition, while may partially recover from donepezil and compound 4e. Subsequently, the further recovery of inhibition by *hu*BuChE inhibitor after dilution was shown in Fig. 2**B**. The *hu*BuChE activity was improved by 0.1 × IC_{50} of rivastigmine from 49.2% (0 min) to 71.8% (240 min), while restored to 98.1% by 0.1 × IC_{50} donepezil at 120 min and still increased to 121.8% at 240 min. Similarly, the 0.1 × IC_{50} of **4e** significantly restored the *hu*BuChE activity to 104.5% until 240 min, which was consistent with 0.1 × IC_{50} donepezil under the same experimental conditions. Hence, compound **4e** was a reversible *hu*BuChE inhibitor.

2.2.3. Inhibition of monoamine oxidases

The inhibitory activities of MAO-A and MAO-B (recombinant human enzyme) were determined via derivatives **4a** ~ **4p** and **5a** ~ **5p**, rasagiline was also evaluated as control [34]. The results exhibited that all the target derivatives displayed weak MAO-A inhibitory potency and some of these derivatives displayed good MAO-B inhibitory potency, especially, compound **4b** showed the best MAO-B inhibitory activity (IC_{50} = 0.9 μM). The SAR indicated that compound **5a** showed potent MAO-B inhibitory potency (IC_{50} = 4.3 μM), when the cinnamic acid fragment of **4a** was replaced with *p*-coumaric acid, (*E*)-3-(thiophen-2-yl) acrylic acid and (*E*)-3-(4-fluorophenyl)acrylic acid to get compounds **4b**, **4e** and **4j**, the MAO-B inhibitory potency significantly increased to 0.9, 1.3 and 3.1 μM, respectively. While when the cinnamic acid fragment of **4a** was replaced with ferulic acid, (*E*)-3-(pyridin-3-yl)acrylic acid, (*E*)-3-(naphthalen-2-yl)acrylic acid, (*E*)-2-methyl-3-phenylacrylic acid, methacrylic acid and 3-phenylpropiolic acid to obtain compounds **4c**, **4d**, **4f, 4 g**, **4 h** and **4i**, the MAO-B inhibitory potency presented different degrees of reduction with IC_{50} values of 7.6, 16.3, 7.5, 22.6, 10.4 and 8.4 μM. Moreover, when the olefin group was reduced, we obtained compounds **4 k**, **4 l** and **4 m**, which showed moderate MAO-B inhibitory potency with IC_{50} values of 9.1, 12.1 and 16.5 μM, respectively. Further, when removing the olefin group, compounds **4n**, **4o** and **4p** were obtained and displayed mild MAO-B inhibitory potency with IC_{50} values of 22.7, 8.1 and 17.9 μM. Accordingly, when the secondary amine was benzylpiperidine, compounds **5a** ~ **5p** displayed moderate to good MAO-B inhibitory potency. Particularly, compounds **5c** and **5 h** showed potent MAO-B inhibitory potency (IC_{50} = 7.9 and 9.1 μM, respectively). The other organic acid have no obvious inhibitory effect on MAO-B.

2.2.4. Antioxidant activity

The oxygen radical absorbance capacity fluorescein (ORAC-FL) assay was employed to evaluate the antioxidant potency, and Trolox (vitamin E analogue) was used as a positive compound [35]. As exhibited in Table 2, target compounds **4a-4p** and **5a-5p** presented moderate to good antioxidant potency with ORAC values ranging from 0.2 *eq* to 1.2 *eq*. In general, the derivatives (**4b**, **4c**, **4 l**, **4 m**, **4o**, **4p**, **5b**, **5c**, **5 k**, **5 l**, **5n** and **5o**) with OH group revealed better antioxidant potency than other derivatives, demonstrating that the OH group served as crucial role for the antioxidant activity. Furthermore, the data indicated that both the organic acid skeleton and secondary amine fragments did not produce significant influence on the antioxidant potency.

2.2.5. Anti-inflammatory property

To evaluate the anti-inflammatory property of cinnamic acid hybrids, compound **4b, 4e** and **5 h** with four different concentration (3.5, 7, 14 and 28 μM) were selected to test the effects on LPS-induced PC12 cell injury using MTT assay [36]. As displayed in Fig. 3, the PC12 cell, which was treated with 1 μg/mL LPS, viability significantly declined to 79.5% ($p < 0.05$) by contrast with untreated group. When treating with compounds **4b** with four different concentration (3.5, 7, 14 and 28 μM), the cell viability remarkably increased to 85.9% ($p < 0.05$), 94.6% ($p < 0.05$), 109.8% ($p < 0.01$) and 96.8% ($p < 0.05$), respectively, in a dose-dependent manner. When treating with compounds **4e** and **5 h**, the similar results were also observed in a dose-dependent manner. The obtained data demonstrated that compound **4b, 4e** and **5 h** indicated

Table 2
In vitro IC_{50} values of of target derivatives toward *hu*MAO-A, *hu*MAO-B, antioxidant activity and inhibition of self-induced A$\beta_{1\text{-}42}$ aggregation.

Comp.	IC_{50} ± SD (μM)[a] *hu*MAO-A	*hu*MAO-B	SI[b]	ORAC[c]	*Inhibition* self-induced A$\beta_{1\text{-}42}$ aggregation[d]
4a	> 50	4.3 ± 0.5	>11.6	0.4 ± 0.01	50.7 ± 2.9
4b	46.9 ± 3.2	0.9 ± 0.02	52.1	1.1 ± 0.02	68.1 ± 3.7
4c	44.6 ± 1.8	7.6 ± 0.3	5.9	1.2 ± 0.03	61.4 ± 4.2
4d	10.5 ± 1.6	16.3 ± 1.3	0.6	0.5 ± 0.02	*n.t.*[e]
4e	21.7 ± 1.3	1.3 ± 0.08	16.7	0.4 ± 0.01	65.2 ± 3.3
4f	27.9 ± 1.8	7.5 ± 0.3	3.7	0.5 ± 0.02	*n.t.*[e]
4 g	23.9 ± 2.2	22.6 ± 1.8	1.1	0.4 ± 0.01	*n.t.*[e]
4 h	15.8 ± 1.4	10.4 ± 0.7	1.5	0.5 ± 0.03	*n.t.*[e]
4i	21.2 ± 1.7	8.4 ± 0.5	2.5	0.4 ± 0.02	*n.t.*[e]
4j	> 50	3.1 ± 0.06	>16.1	0.3 ± 0.02	*n.t.*[e]
4 k	> 50	9.1 ± 0.3	>5.5	0.6 ± 0.03	*n.t.*[e]
4 l	> 50	12.1 ± 1.8	>4.1	1.2 ± 0.03	*n.t.*[e]
4m	> 50	16.5 ± 1.3	3	1.1 ± 0.05	*n.t.*[e]
4n	> 50	22.7 ± 1.6	2.2	0.5 ± 0.02	*n.t.*[e]
4o	> 50	8.1 ± 0.6	>6.2	1.2 ± 0.03	*n.t.*[e]
4p	> 50	17.9 ± 0.8	>2.8	1.3 ± 0.05	*n.t.*[e]
5a	> 50	27.5 ± 1.3	>1.8	0.5 ± 0.03	*n.t.*[e]
5b	> 50	11.9 ± 1.1	>4.2	1.1 ± 0.02	*n.t.*[e]
5c	> 50	7.9 ± 0.2	>6.3	1.2 ± 0.04	*n.t.*[e]
5d	> 50	11.9 ± 1.6	>4.2	0.4 ± 0.02	*n.t.*[e]
5e	15.7 ± 1.1	11.5 ± 0.9	1.4	0.5 ± 0.06	*n.t.*[e]
5f	29.4 ± 1.8	15.8 ± 0.6	1.9	0.6 ± 0.02	*n.t.*[e]
5g	29.1 ± 1.9	11 ± 0.8	2.6	0.5 ± 0.01	*n.t.*[e]
5h	> 50	9.1 ± 0.2	>5.5	0.4 ± 0.02	70.3 ± 5.3
5i	> 50	11.7 ± 0.7	>4.3	0.3 ± 0.02	*n.t.*[e]
5j	> 50	> 50	—	0.5 ± 0.04	*n.t.*[e]
5 k	30.3 ± 1.9	25.1 ± 2.3	1.2	1.2 ± 0.02	*n.t.*[e]
5l	22.1 ± 1.6	47.3 ± 3.7	0.5	1.1 ± 0.04	*n.t.*[e]
5m	35.2 ± 2.2	21.6 ± 1.9	1.6	0.5 ± 0.03	*n.t.*[e]
5n	28.2 ± 2.3	10.7 ± 0.2	2.6	1.1 ± 0.04	*n.t.*[e]
5o	> 50	10.8 ± 1.4	>4.6	1.2 ± 0.02	*n.t.*[e]
5p	> 50	> 50	1	0.2 ± 0.01	*n.t.*[e]
rasagiline	0.59 ± 0.04	0.029 ± 0.002	20.3	*n.t.*[e]	*n.t.*[e]
curcumin	*n.t.*[e]	*n.t.*[e]	*n.t.*[e]	*n.t.*[e]	40.3 ± 2.8

[a] Three experiments were performed and expressed as means ± SD.
[b] SI = Selectivity Index = IC_{50} (MAO-A) / IC_{50} (MAO-B).
[c] data are presented as μM of Trolox equiv/μM of measured compound.

[d] Inhibition of self-induced A$\beta_{1\text{-}42}$ aggregation, three independent experiments were carried out and presented as the mean ± SEM, the concentration of tested compounds and A$\beta_{1\text{-}42}$ were 25 μM.

[e] *n.t. = not tested*

significant anti-inflammatory property.

2.2.6. Inhibition of self-induced Aβ_{1-42} aggregation

Based on the results from the ChEs inhibition assay and MAOs inhibition assay, the promising compounds **4a**, **4b**, **4c**, **4e** and **5 h** were selected to test the inhibition effects against self-induced Aβ_{1-42} aggregation by thioflavin T (ThT) fluorescence assay using curcumin as positive control [33,35]. Based on the data in Table 1, compounds **4a**, **4b**, **4c**, **4e** and **5 h** showed significant inhibitory potency against self-induced Aβ_{1-42} aggregation with 50.7%, 68.1%, 61.4%, 65.2% and 70.3% inhibition rate at 25 μM, which were better than curcumin (40.3%).

2.2.7. Transmission electron microscopy (TEM)

Compound **4e** was selected to evaluate and further supplement the inhibition of self-induced A$\beta_{1\text{-}42}$ aggregation by TEM using curcumin as a control compouond [33,35]. As displayed in Fig. 4, the fresh A$\beta_{1\text{-}42}$ gradually agglomerated into fibrils after 24 h of culture, while small fibril agglomerates were presented after treating compounds **4e** and curcumin, respectively. The TEM images suggest that **4e** significantly inhibit self-induced A$\beta_{1\text{-}42}$ aggregation, which was consistent with the ThT assay.

2.2.8. Neuroprotective effects against Aβ-induced SH-SY5Y cell toxicity

To determine the potential cytotoxic effects of compound **4e** on neuronal cell line SH-SY5Y, the most promising compound **4e** was selected for treatment, with different concentrations ranging from 1 to 100 μM [37]. After exposing the SH-SY5Y cells to compound **4e** for 48 h, the cell viability was assessed by 3-(4,5-dimethylthiazol-2-yl)-2,5-diphenyltetrazolium (MTT) assay. Fig. 5**A** displayed compound **4e** did not present obvious cytotoxic effect on the SH-SY5Y cells at 50 μM.

To consolidate the results obtained from A$\beta_{1\text{-}42}$-induced inhibition studies, further study was performed to evaluate the neuroprotective effect of **4e** against SH-SY5Y cell injury induced by A$\beta_{1\text{-}42}$ using MTT assay [37]. Three different concentration of **4e** (5, 10 and 20 μM) were used in this experiment. As displayed in Fig. 5**B**, treatment with 25 μM A$\beta_{1\text{-}42}$ for 48 h. Compared with the control group, the cell viability decreased to 47.5% ($p < 0.01$). Compound **4e**, significantly increased the cell viability to 60.5%, 67.8% and 69.6% in a dose-dependent manner, showing a promising neuroprotective effect against SH-SY5Y cell toxicity induced by A$\beta_{1\text{-}42}$.

2.2.9. Molecular modeling study

To explore the combination of **4e** with *hu*BuChE and *hu*MAO-B, the human BuChE (PDB code: 4tpk) and human MAO-B (PDB code: 2 V60) were applied to do molecular docking [33,34].

As presented in Fig. 6, the results displayed that **4e** interacted with *hu*BuChE through multiple sites. In the *hu*BuChE-**4e** complex (Fig. 6**A** ~ **6C**), the benzene ring of 1,2,3,4-tetrahydroisoquinoline interacted with key residue Trp82 *via* two Pi-Pi interactions, the alkylene interacted with key residue Trp82 through Sigma-Pi interaction, and the thiophene ring interacted with important residue Trp430 through two Pi-Pi interactions. In addition, compound **4e** has hydrophobic interaction with residueTrp82, Ala328, Tyr128, Tyr440, Gly439, Gly121, Trp430 and Thr120. Therefore, the observed ligand-residue interaction offered the possible explain for potent *hu*BuChE inhibitory potency.

To explore the combination of **4e** with human MAO-B (PDB code: 2 V60), a docking was employed. In **4e**-MAO-B complex (Fig. 7), the O atom of carbonyl group interacted with key residue Thr 314 through one intermolecular hydrogen bonding, and the thiophene ring interacted with Val82 and Leu328 *via* one Sigma-Pi interaction, respectively. Moreover, some hydrophobic interactions were observed between the compound **4e** and residue Pro102, Leu88, Glu84, Val82, Thr314, and Leu328 in MAO-B. Therefore, the obtained phenomenon might provide explanation for the potent MAO-B inhibitory potency.

2.2.10. In vitro BBB permeation assay

Parallel artificial membrane permeation assay was used to evaluate the ability of **4e** for permeating blood–brain barrier (BBB) [38,39]. 11 control drugs were used as the references. The following ranges of permeability P_e ($\times 10^{-6}$ cm/s) had been established based on our

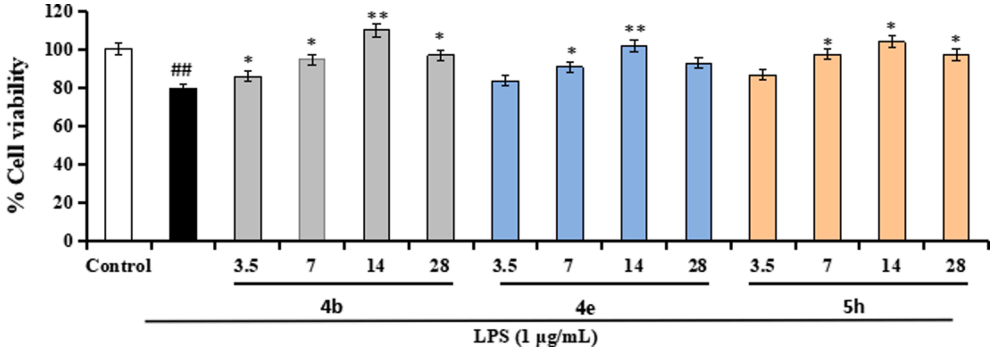

Fig. 3. The cell viability (%) of compound **4e** on LPS-induced PC12 cell injury by MTT assay. The data were expressed as mean ± SD from three independent experiments. ##p < 0.01 vs control group; **$p < 0.01$, *$p < 0.05$ vs LPS-induced group.

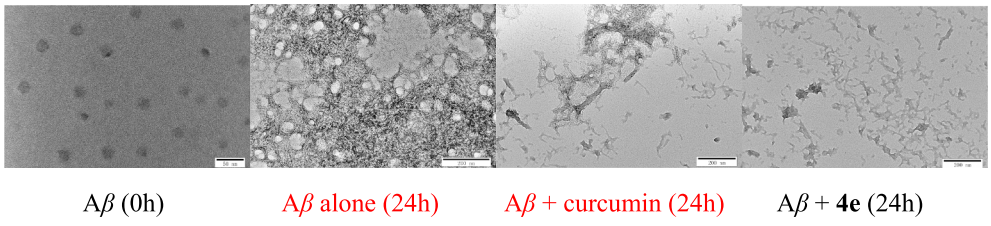

Fig. 4. TEM images of Aβ species from inhibition experiments.

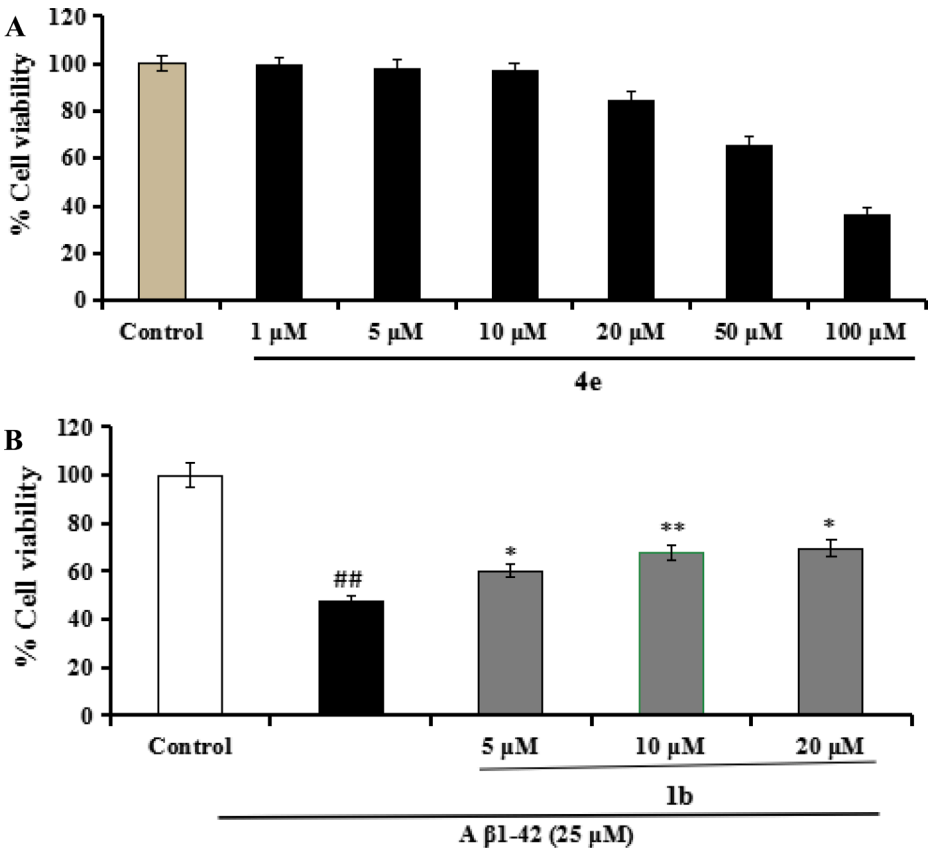

Fig. 5. (A) effect of compound **4e** on the viability of SH-SY5Y cells by MTT assay. (B) The cell viability (%) of **4e** on A$\beta_{1\text{-}42}$-induced SH-SY5Y cell toxicity via MTT assay. Percentages of the cell viability were presented as mean ± SD from three independent experiments. ##p < 0.01 vs untreated control; **$p < 0.01$, *$p < 0.05$ vs A group.

previous work: $P_e > 3.44$ for compounds with predicted high BBB permeation. The results in Table 3 showed that compound **4e** exhibited 11.67×10^{-6} cm/s permeability, as similar with verapamil and verapamil, revealing that compound **4e** could cross the BBB by passive diffusion.

2.2.11. Prediction of druglike properties

The Molinspiration property program was used to predict the druglike properties. The items containing log *P*, molecular weight (MW), topological polar surface area (TPSA), number of hydrogen-bond acceptors (*n*-ON), number of hydrogen-bond donors (*n*-OHNH) [40]. As displayed in Table 4**e** complied with the Lipinski's rule of five, deserving for further *in vivo* experiments.

*2.2.12. Effect of **4e** on $AlCl_3$-induced zebrafish AD*

Zebrafish AD induced by $AlCl_3$ has been widely employed to discover novel agents to treat AD [33,35,41].

(1) *Acute toxicity*. To determine the safety of **4e**, six concentrations of **4e** (2.0, 4.0, 8.0, 16.0 and 32.0 μg/mL) and vehicle group (1% DMSO) were employed to treat 2dpf zebrafish. The results revealed that the maximum non-lethal concentration (MNLC) of **4e** was 8.0 μg/ mL. Then, three different concentrations of **4e** (0.9, 2.7 and 8.0 μg/mL), untreated group and vehicle group were used to treat 2dpf zerbrafish for 3 days. As listed in **Table S1**, treatment with MNLC/9 (0.9 μg/mL) **4e** did not present any toxicity, except induced 16.7% yolk sac absorption delay. Treatment with MNLC/3 (2.7 μg/mL) **4e** induced 40% yolk sac absorption delay and 26.7% pericardial edema. Treatment with MNLC (8.0 μg/mL) **4e** induced 100% yolk sac absorption delay, 76.7% pericardial edema, 66.7% short or misshapen jaw, 60% kidney edema, 53.3% small or misshapen eye(s), 53.3% degenerating muscle within the somites, 46.7% presence of dark brown, 46.7% body shape, 33.3% small and misshapen brain, 16.7% absent blood flow and slow blood flow, and 6.7% death.

(2) Assessing assay on zebrafish AD induced by $AlCl_3$. The change experiments of distance and speed were performed to assess the dyskinesia and reaction capacity of compound **4e** on zebrafish AD induced by $AlCl_3$.

Based on the result from **Table S2**, the MTC (maximum tolerated concentration) of **4e** was 0.8 μg/mL. Three different concentrations of **4e** (0.2 μg/mL, 0.4 μg/mL and 0.8 μg/mL), donepezil group (DPZ, 8.0 μM), untreated zebrafish and $AlCl_3$-induced zebrafish AD were used in this experiments. As indicated in Fig. 8**A**, when zebrafish were treated with $AlCl_3$, the distance remarkably declined to 5249 mm ($p < 0.01$) compared to untreated group (7326 mm). While the distance increased to 6408 mm (DPZ group, $p < 0.01$) treating with 8.0 μM donepezil in contrast to model group. Moreover, treatment with three different concentrations of compound **4e** (0.2 μg/mL, 0.4 μg/mL and 0.8 μg/mL), the distance gradually increased to 6125 mm ($p < 0.05$), 6501 mm ($p < 0.01$) and 6932 mm ($p < 0.01$), respectively, in a dose-dependent manner. Particularly, the high dose of **4e** (0.8 μg/mL) presented longer distance than donepezil.

Subsequently, in Fig. 8**B**, speed change of AD zebrafish induced by $AlCl_3$ (model group) was significantly lower (1.07 mm/s) than the untreated group (2.32 mm/s, P < 0.001). When treating with 8.0 μM donepezil (DZP group), the speed change added up to 1.87 mm/s ($p < 0.01$). Meanwhile, treating with three different concentrations of **4e** , the number of speed change gradually increased to 1.67 ($p < 0.05$), 1.81 ($p < 0.01$) and 2.16 mm/s ($p < 0.05$) in a dose-dependent manner, and the high dose (0.8 μg/ mL) demonstrated better speed change than

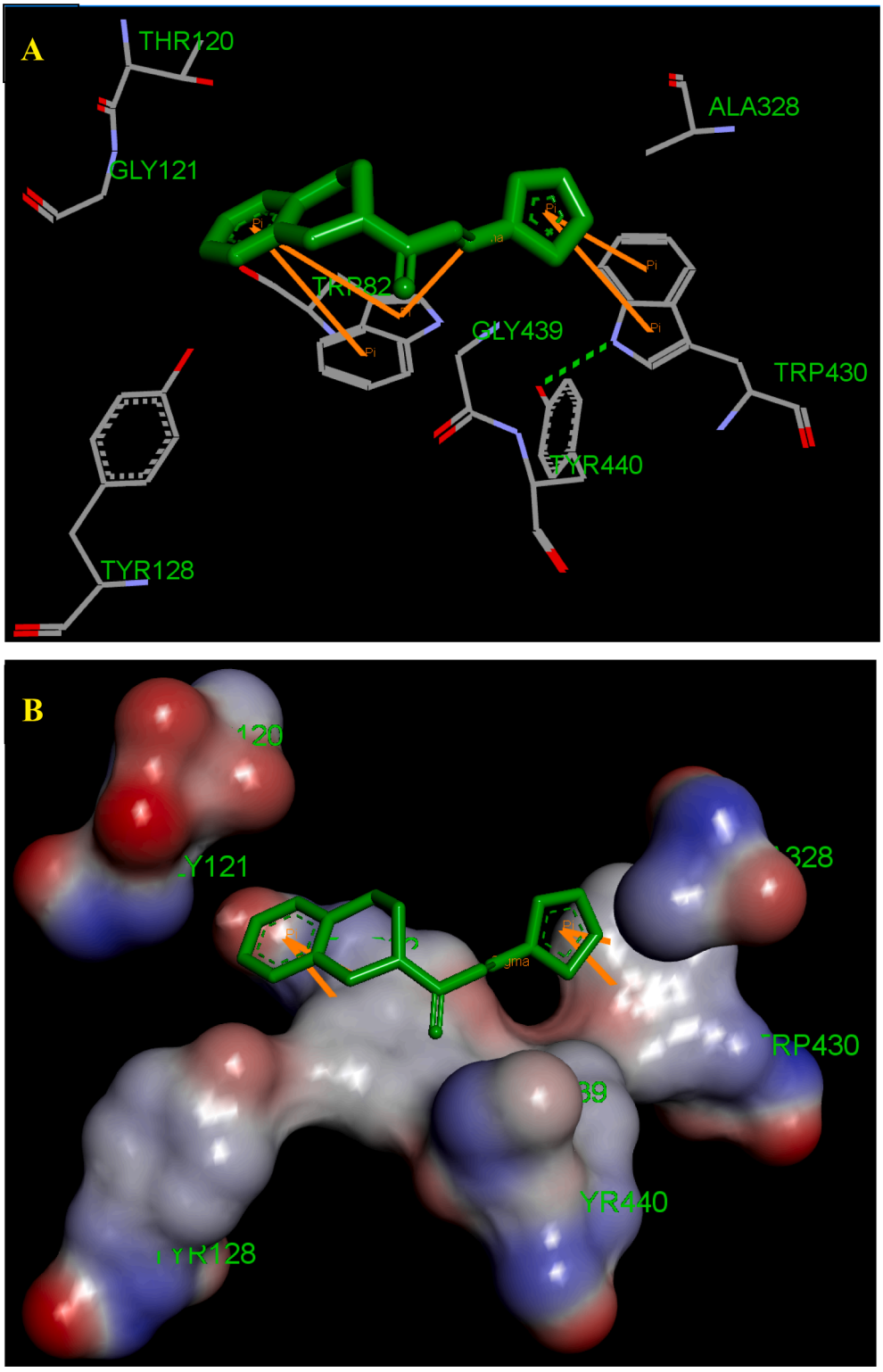

Fig. 6. Compound **4e** (green stick) interacting with residues in the binding site of *hu*BuChE (PDB code: 4tpk). (A) Show ligand binding site atoms; (B) Create surface around ligand; (C) Show 2D diagram.

donepezil.

*2.2.13. The effect of **4e** on scopolamine-induced memory impairment*

To determine the safety profile of compound **4e**, the acute toxicity experiments were performed by oral administration of compound **4e** at doses of 500, 1000, and 1500 mg/kg (n = 10 / group) using Kunming mice at body weight of 18–22 g. The results showed that the animals did not show any acute toxicity after oral administrating compound **4e** for 14 days at doses up to 1500 mg/kg.

The step-down passive avoidance task was employed to test the effects of **4e** on mice memory impairment induced by scopolamine [33,35]. Three different concentration of **4e** (50, 10 and 2 mg/kg) were

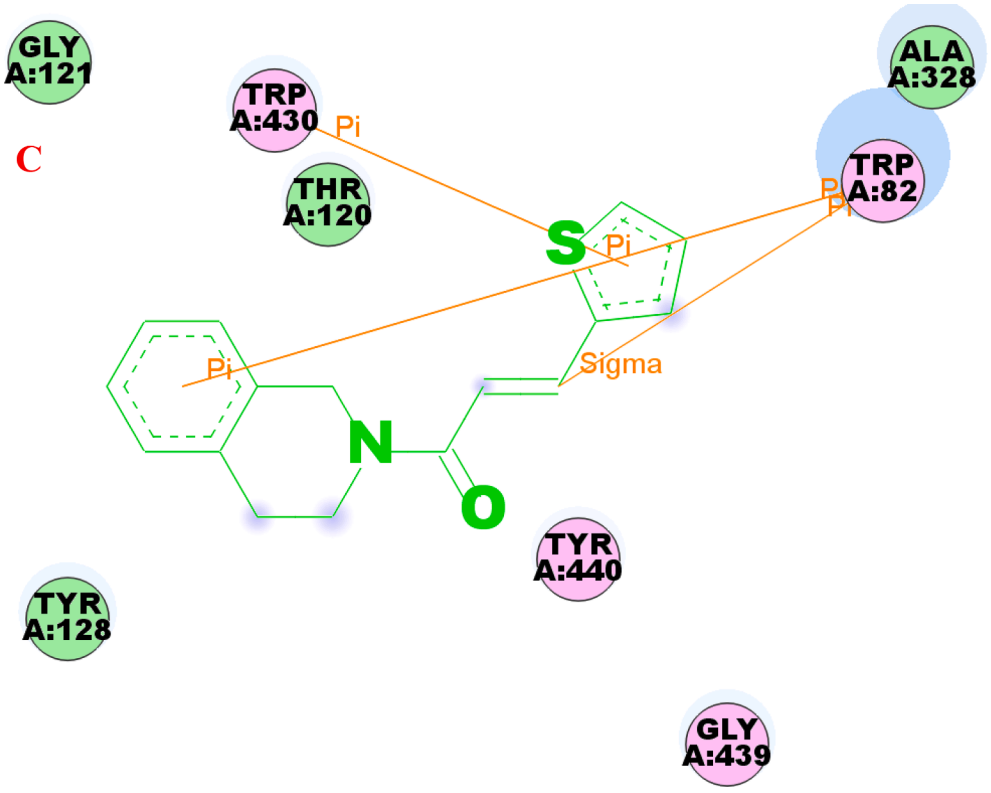

Fig. 6. (*continued*).

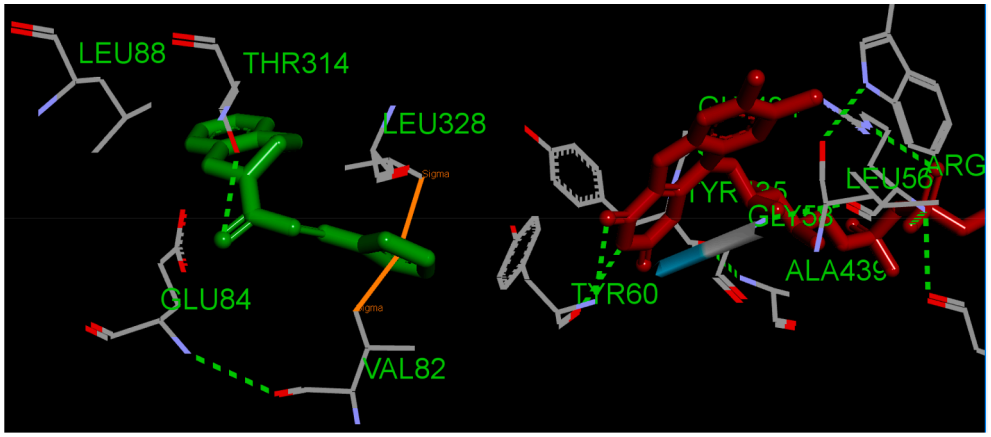

Fig. 7. **4e** (green stick) interacted with the binding site of *hu*MAO-B (PDB code: 2 V60). (For interpretation of the references to colour in this figure legend, the reader is referred to the web version of this article.)

Table 3
Permeability P_e ($\times 10^{-6}$ cm/s) of compounds **4e,** verapamil and verapamil by PAMPA-BBB assay and the predictive penetration in the CNS.

Compound[a]	P_e ($\times 10^{-6}$ cm/s)	Prediction
4e	11.67 ± 0.82	CNS +
verapamil	15.67 ± 0.89	CNS+
diazepam	12.53 ± 0.61	CNS+

[a] Compounds **4e,** verapamil and verapamil were dissolved in DMSO at 5 mg/mL and diluted with PBS/EtOH (70:30), respectively. The final concentration of the compound was 100 μg/mL.

used in this experiment, and 14.0 mg/kg donepezil served as positive compound. As presented in Fig. 9, the mice were treated with 2 mg/kg scopolamine alone, the step-down latency significantly declined to 130.3 ($p < 0.01$) compared with untreated group (239.1 *sec*). Then treatment with 14.0 mg/kg donepezil, the latency time significantly added up to 171.8 *sec* ($p < 0.05$) and significantly improved scopolamine-induced cognitive deficit. Moreover, treatment with three concentrations of compound **4e** (50, 10 and 2 mg/kg), the latency time added up to 170.2 *sec* ($p < 0.05$), 180.7 *sec* ($p < 0.05$) and 212.1 *sec* ($p < 0.01$), respectively. The obtained results reveal that compound **4e** significantly improved memory impairment induced by scopolamine, and the high dose presented better effects than donepezil. Thus, compound **4e** deserved to further investigation *in vivo*.

2.2.14. *The stability studies of **4e** in artificial gastrointestinal fluid*

The stability of **4e** was evaluated using artificial gastrointestinal fluid [42]. As presented in Table 5 and Fig. 10, compound **4e** was stable in both artificial gastric fluid and artificial intestinal fluid, and it was more

Table 4
Theoretical prediction of the ADME properties of compound **4e.**

Comp.[a]	Log *P*	MW	TPSA (Å^2)	*n*-ON	*n*-OHNH	nviolations	nrotb	volume (Å^3)
4e	3.12	269.37	20.31	2	0	0	2	44.91

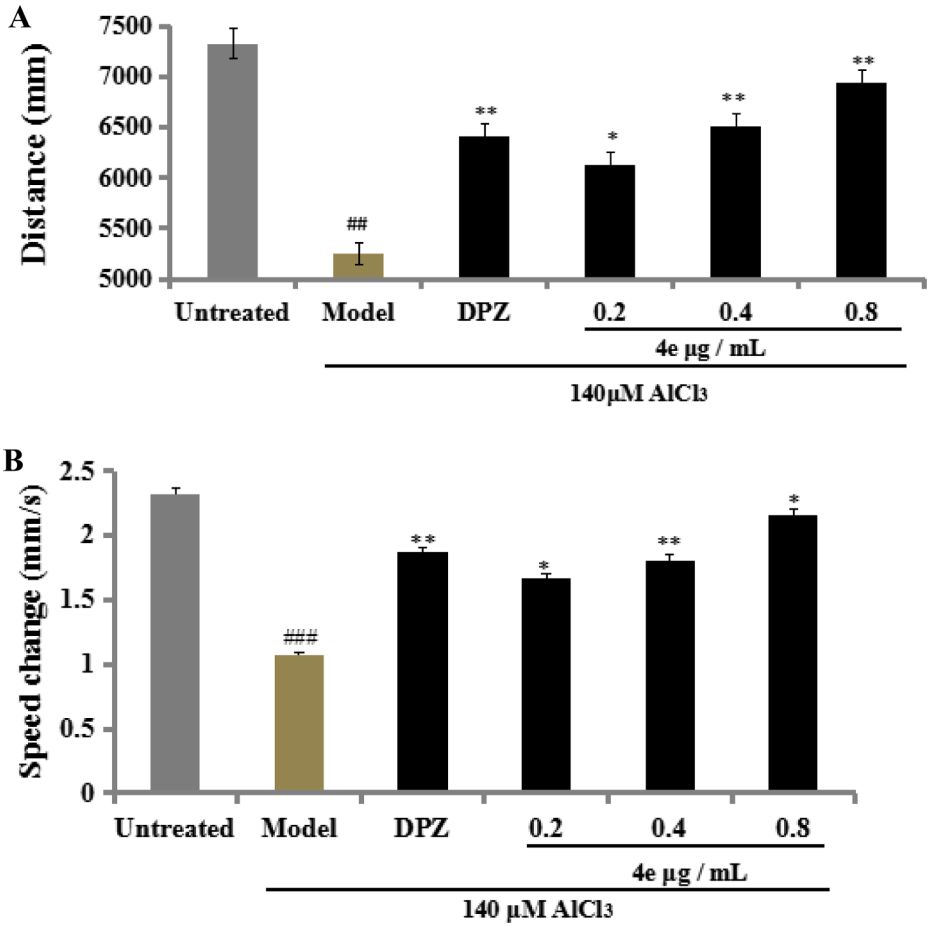

Fig. 8. (A) The motility distance of **4e** in zebrafish experiments. (B) Speed change of **4e** on speed change in zebrafish experiments. $##p < 0.01$, $###p < 0.001$ vs. untreated group; $*p < 0.05$, $**$ $p < 0.01$ vs model group.

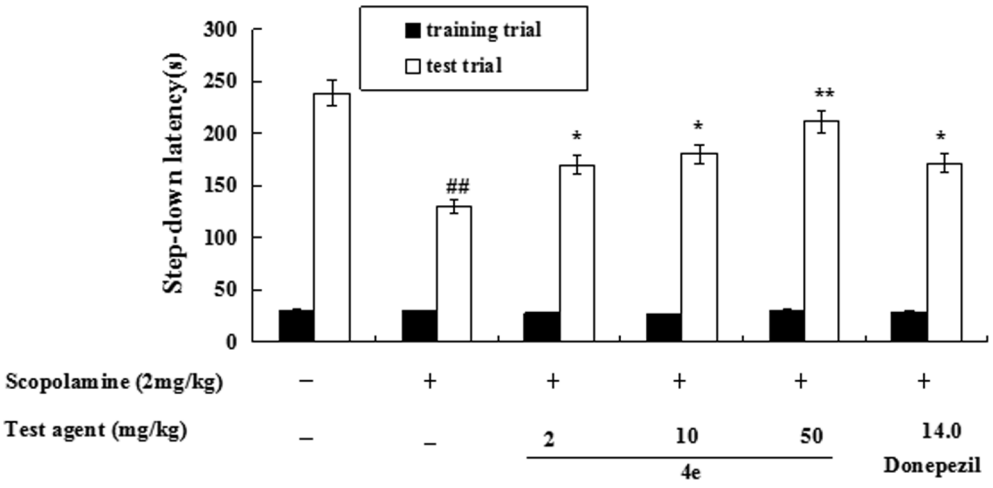

Fig. 9. Effects of **4e** on mice memory impairment induced by scopolamine. The data are presented as mean ± SD (n = 10). $^{##}p < 0.01$ vs untreated group. $*p < 0.05$ and $**p < 0.01$ vs scopolamine-treated group.

Table 5
The Stability of **4e** in Artificial Gastrointestinal Fluid (1 mg/mL, n = 3).

Time (h)	Blank gastric fluid (%)	Artificial gastric fluid (%)	Blank intestinal fluid (%)	Artificial intestinal fluid (%)
0	100.00 ± 4.54	100.00 ± 2.2	100.00 ± 3.48	100.00 ± 2.10
0.5	92.26 ± 1.21	90.99 ± 0.68	89.76 ± 0.31	90.88 ± 1.57
1	86.90 ± 1.59	85.46 ± 1.72	83.37 ± 5.11	85.93 ± 1.10
2	77.32 ± 1.53	75.16 ± 1.71	73.33 ± 1.93	74.49 ± 1.04
3	73.57 ± 0.81	68.71 ± 0.91	68.94 ± 1.91	67.28 ± 2.52
4	65.05 ± 2.11	63.40 ± 0.90	69.95 ± 0.86	58.96 ± 1.28
6	59.25 ± 7.19	57.95 ± 2.44	53.72 ± 2.61	51.32 ± 0.77
8	50.66 ± 2.20	52.95 ± 2.17	49.58 ± 2.95	45.40 ± 2.77

stable in artificial gastric fluid than in artificial intestinal fluid.

3. Conclusion

A series of novel cinnamic acid hybrids were designed and synthesized by the MTDLs approach. Based on *in vitro* biological activity evaluation, **4e** was the best one which was a reversible *hu*BuChE inhibitor (IC_{50} = 2.5 μM). Compound **4e** also exhibited good MAO-B inhibition activity (IC_{50} = 1.3 μM) and antioxidant potency (ORAC = 0.4 eq). Moreover, compound **4e** significantly inhibited self-mediated A$\beta_{1\text{-}42}$ aggregation (65.2%). Compound **4e** exhibited remarkable anti-inflammatory potency and neuroprotective effect. Furthermore, compound **4e** presented favourable BBB penetration. Further, compound **4e** significantly improved dyskinesia recovery rate and response efficiency on $AlCl_3$-induced zebrafish and improved scopolamine-induced memory impairment. More interesting, compound **4e** presented good stability in both artificial gastric fluid and artificial intestinal fluid. Therefore, compound **4e** would be a potent multi-targeted active molecule against AD.

4. Experiments

4.1. Chemistry

All reagents were commercially sourced and used without further purification. ^{1}H NMR and ^{13}C NMR spectra were recorded at 400 and 100 MHz, respectively, on a Varian INOVA spectrometer and used $CDCl_3$ or DMSO-d_6 as solvents, referenced to Tetramethylsilane (TMS). Chemical shifts (δ) are reported in ppm. Splitting patterns are designated as s, single; d, doublet; dd, double-doublet; t, triplet; m, multiplet. The high-resolution mass spectra was obtained by Waters Xevo G2-XS-Qtof mass spectrometer. The purity of all final compounds were determined by waters 2695 High Performance Liquid Chromatography (HPLC) with a Waters X-Bridge C18 column (4.6 mm × 150 mm, 5 μm) at a flow ratio of 0.8 mL/min. Mobile phase: A: 0.12%TFA in H_2O, B: 0.1% TFA in CH_3CN.

4.1.1. General procedure for the preparation of cinnamic acid hyrbids **4a-4p** and **5a-5p**

The starting materials **1a-1q** (1 mmol) were dissolved in anhydrous dichloromethane (8 mL), respectively. EDCI) (1.5 mmol) and HOBt (1.5 mmol) were added to the solution as condensating agent. Finally, the excessive amounts of 1,2,3,4-tetrahydroisoquinoline (**a**) and 4-benzylpiperidine (**b**) (1 ~ 2 mmol) was added to the aforementioned solution, respectively. The reaction mixture was stirred under room temperature for 6 ~ 8 h monitored by TLC. After reaction finished, the mixture was diluted with water and extracted with CH_2Cl_2. The organic phases were combined, washed with saturated aqueous $NaHCO_3$ and brine, dried over Na_2SO_4, filtered, and evaporated *in vacuo*. The residue was purified by silica gel chromatography with dichloromethane/acetone = 50:1 as eluent to give the target compounds **4a**-**4p** and **5a**-**5p**.

*4.1.1.1. (E)-1-(3,4-dihydroisoquinolin-2(1H)-yl)-3-phenylprop-2-en-1-one (**4a**).* Yellow oil, 68.9% yield, 97.6% HPLC purity. ^{1}H NMR (400 MHz, $CDCl_3$) δ 7.84 (d, *J* = 15.1 Hz, 1H, C = CH), 7.31 (d, *J* = 4.6 Hz, 1H, Ar-H), 7.20 (m, 7H, 7 × Ar-H), 7.03 (m, 1H, Ar-H), 6.75 (d, *J* = 15.1 Hz, 1H, C = CH), 4.81 (s, 2H, NCH_2), 3.86 (d, *J* = 29.2 Hz, 2H, NCH_2), 2.92 (s, 2H, CH_2). HR-ESI-MS: Calcd. for $C_{18}H_{17}NO$ $[M + H]^+$: 264.1383, found: 264.1393.

*4.1.1.2. (E)-1-(3,4-dihydroisoquinolin-2(1H)-yl)-3-(4-hydroxyphenyl) prop-2-en-1-one (**4b**).* Yellow oil, 76.7% yield, 97.4% HPLC purity. ^{1}H NMR (400 MHz, $CDCl_3$) δ 7.64 (d, *J* = 15.2 Hz, 1H, CH = CH), 7.36 (d, *J* = 7.6 Hz, 2H, 2 × Ar-H), 7.20–7.11 (m, 4H, 4 × Ar-H), 6.90 (d, *J* = 8.4 Hz, 1H, 2 × Ar-H), 6.75 (d, *J* = 15.2 Hz, 1H, CH = CH), 4.83 (s, 2H, $phCH_2$), 3.85–3.82 (m, 2H, $phCH_2$), 2.95–2.89 (m, 2H, $phCH_2$). ^{13}C NMR (100 MHz, $CDCl_3$) δ 174.5, 158.7, 143.6, 129.7, 127.0, 126.7, 116.1, 113.8, 45.0, 43.8, 40.6. HR-ESI-MS: Calcd. for $C_{18}H_{17}NO_2$ $[M + H]^+$: 280.1332, found: 280.1345.

*4.1.1.3. (E)-1-(3,4-dihydroisoquinolin-2(1H)-yl)-3-(4-hydroxy-3-methoxyphenyl)prop-2-en-1-one (**4c**).* Yellow oil, 51.6% yield, 97.8% HPLC purity. ^{1}H NMR (400 MHz, $CDCl_3$) δ 7.65 (d, *J* = 15.2 Hz, 1H, CH = CH), 7.19–7.11 (m, 5H, 5 × Ar-H), 7.01 (s, 1H, Ar-H), 6.93 (d, *J* = 8.0 Hz, 1H, Ar-H), 6.79 (d, *J* = 15.6 Hz, 1H, CH = CH), 6.16–6.04 (brs, 1H, OH), 4.83 (s, 2H, $phCH_2$), 3.93 (s, 3H, OCH_3), 3.90–3.87 (m, 2H, $phCH_2$), 2.96–2.92 (m, 2H, NCH_2). ^{13}C NMR (100 MHz, $CDCl_3$) 166.2, 147.4, 146.7, 143.1, 134.3, 133.7, 128.97, 128.3, 127.8, 126.8, 126.1, 121.9,

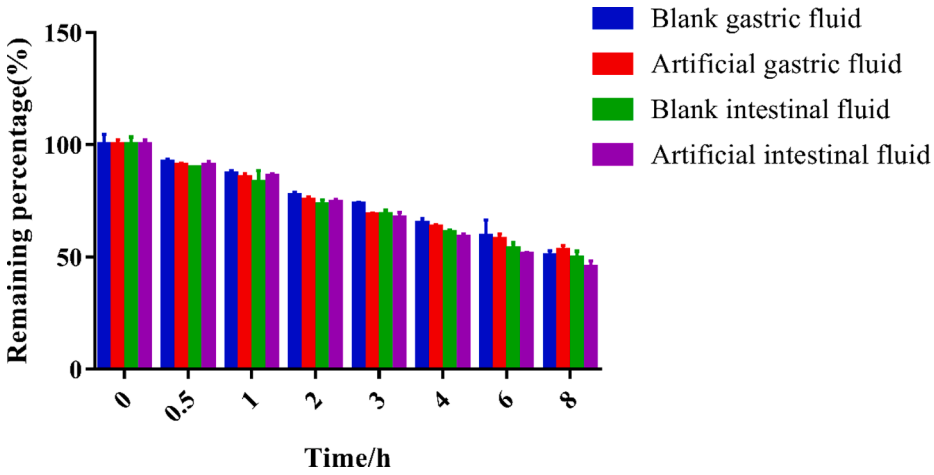

Fig. 10. The remaining percentage (%) of **4e** in artificial gastrointestinal fluid (1 mg/mL, n = 3).

114.8 (2C), 110.0, 56.0, 43.6, 29.7. HR-ESI-MS: Calcd. for $C_{19}H_{19}NO_3$ $[M + H]^+$: 310.1438, found: 310.1447.

*4.1.1.4. (E)-1-(3,4-dihydroisoquinolin-2(1H)-yl)-3-(pyridin-3-yl)prop-2-en-1-one (**4d**).* Yellow oil, 81.7% yield, 98.1% HPLC purity. ^{1}H NMR (400 MHz, $CDCl_3$) δ 8.75 (s, 1H, OH), 8.54 (d, J = 4.4 Hz, 1H, Ar-H), 7.84 (d, J = 7.6 Hz, 1H, Ar-H), 7.67 (d, J = 15.2 Hz, 1H, Ar-H), 7.31–7.25 (m, 1H, Ar-H), 7.16 (d, J = 13.2 Hz, 4H, 4 × Ar-H), 7.07 (d, J = 15.2 Hz, 1H, CH = CH), 4.82 (s, 2H, phCH2), 3.90–3.85 (m, 2H, phCH2), 2.94–2.87 (m, 2H, NCH2). ^{13}C NMR (100 MHz, $CDCl_3$) δ 165.1, 150.1 (2C), 149.1, 138.9, 134.3 (2C), 131.0, 126.6, 123.7 (2C), 44.8, 43.6, 29.5. HR-ESI-MS: Calcd. for $C_{17}H_{16}N_2O$ $[M + H]^+$: 265.1335, found: 265.1352.

*4.1.1.5. (E)-1-(3,4-dihydroisoquinolin-2(1H)-yl)-3-(thiophen-2-yl)prop-2-en-1-one (**4e**).* Light yellow oil, 70.7% yield, 97.4% HPLC purity. ^{1}H NMR (400 MHz, $CDCl_3$) δ 7.85 (d, J = 15.1 Hz, 1H, C = CH), 7.32 (d, J = 5.1 Hz, 1H, Ar-H), 7.23 (d, J = 3.8 Hz, 1H, Ar-H), 7.20 (m, 2H, 2 × Ar–H), 7.18 (d, J = 3.1 Hz, 2H, 2 × Ar–H), 7.04 (dd, J = 5.0, 3.7 Hz, 1H, Ar-H), 6.75 (d, J = 15.1 Hz, 1H, C = CH), 4.83 (s, 2H, NCH_2), 3.88 (d, J = 30.2 Hz, 2H, NCH_2), 2.95 (s, 2H, CH_2). ^{13}C NMR (100 MHz, $CDCl_3$) δ 165.7, 140.6, 135.7 (2C), 130.4 (2C), 128.1 (2C), 127.3, 126.8, 126.8, 126.7, 116.3, 45.0, 43.7, 29.8. HR-ESI-MS: Calcd. for $C_{16}H_{15}NOS$ $[M + H]^+$: 270.0947, found: 270.0955.

*4.1.1.6. (E)-1-(3,4-dihydroisoquinolin-2(1H)-yl)(naphthalen-2-yl)methanone (**4f**).* Yellow oil, 59.7% yield, 97.5% HPLC purity. ^{1}H NMR (400 MHz, $CDCl_3$) δ 8.43 (d, J = 15.2 Hz, 1H, CH = CH), 8.11 (d, J = 7.9 Hz, 1H, Ar-H), 7.74 (d, J = 7.9 Hz, 2H, 2 × Ar-H), 7.62 (d, J = 6.8 Hz, 1H, Ar-H), 7.39 (m, 3H, 3 × Ar-H), 7.08 (t, J = 17.7 Hz, 4H, 3 × Ar-H, CH = CH), 6.89 (dd, J = 14.7, 8.5 Hz, 1H, Ar-H), 4.74 (d, J = 21.9 Hz, 2H, NCH_2), 3.80 (d, J = 42.9 Hz, 2H, NCH_2), 2.81 (s, 2H, CH_2). HR-ESI-MS: Calcd. for $C_{22}H_{19}NO$ $[M + H]^+$: 314.1539, found: 314.1547.

*4.1.1.7. (E)-1-(3,4-dihydroisoquinolin-2(1H)-yl)-3-phenylbut-2-en-1-one (**4 g**).* Yellow oil, 77.2% yield, 97.7% HPLC purity. ^{1}H NMR (400 MHz, $CDCl_3$) δ 7.40–7.33 (m, 4H, 4 × Ar-H), 7.31–7.26 (m, 1H, Ar-H), 7.21–7.11 (m, 4H, 4 × Ar-H), 6.59 (s, 1H, Ar-H), 4.77 (s, 2H, $phCH_2$), 3.87–3.82 (m, 2H, $phCH_2$), 2.91 (t, J = 6.0 Hz, NCH_2), 2.14 (s, 3H, CH_3). ^{13}C NMR (100 MHz, $CDCl_3$) δ 172.9, 136.0, 133.2, 133.1, 129.8, 129.1, 129.0 (2C), 128.8, 128.4 (2C), 128.3, 127.5, 126.7, 126.5, 44.8, 29.7, 29.5, 16.1. HR-ESI-MS: Calcd. for $C_{19}H_{19}NO$ $[M + H]^+$: 278.1539, found: 278.1551.

*4.1.1.8. 1-(3,4-dihydroisoquinolin-2(1H)-yl)-2-methylprop-2-en-1-one (**4 h**).* Yellow oil, 78.5% yield, 98.2% HPLC purity.^{1}H NMR (400 MHz, $CDCl_3$) δ 7.15 (d, J = 13.0 Hz, 4H, 4 × Ar-H), 5.23 (s, 1H, 1/2C = CH_2), 5.09 (s, 1H, 1/2C = CH_2), 4.71 (d, J = 24.9 Hz, 2H, NCH_2), 3.79 (d, J = 35.3 Hz, 2H, NCH_2), 2.87 (s, 2H, CH_2), 1.95 (d, J = 28.6 Hz, 3H, CH_3). HR-ESI-MS: Calcd. for $C_{13}H_{15}NO$ $[M + H]^+$: 202.1226, found: 202.1241.

*4.1.1.9. 1-(3,4-dihydroisoquinolin-2(1H)-yl)-3-phenylprop-2-yn-1-one (**4i**).* Yellow oil, 69.4% yield, 97.7% HPLC purity. ^{1}H NMR (400 MHz, $CDCl_3$) δ 7.66 (d, J = 15.2 Hz, 1H, CH = CH), 7.52 (d, J = 5.6 Hz, 2H, 2 × Ar-H), 7.18–7.15 (m, 4H, 4 × Ar-H), 7.04 (t, J = 8.4 Hz, 2H, 2 × Ar-H), 6.88 (d, J = 15.2 Hz, 1H, CH = CH), 4.81 (s, 2H, $phCH_2$), 3.88 (d, J = 24.0 Hz, 2H, $phCH_2$), 2.94–2.92 (m, 2H, NCH_2). ^{13}C NMR (100 MHz, $CDCl_3$) δ 164.7, 141.5, 131.6, 131.5, 129.7 (2C), 129.6 (2C), 128.3, 126.7, 117.3, 116.0 (2C), 115.8 (2C), 44.8, 43.6, 29.7. HR-ESI-MS: Calcd. for $C_{18}H_{15}NO$ $[M + H]^+$: 262.1226, found: 262.1234.

*4.1.1.10. (E)-1-(3,4-dihydroisoquinolin-2(1H)-yl)-3-(4-fluorophenyl) prop-2-en-1-one (**4j**).* Light yellow oil, 75.8% yield, 97.3% HPLC purity. ^{1}H NMR (400 MHz, $CDCl_3$) δ 7.66 (d, J = 15.2 Hz, 1H, CH = CH), 7.52 (d, J = 5.6 Hz, 2H, 2 × Ar-H), 7.18–7.15 (m, 4H, 4 × Ar-H), 7.04 (t, J = 8.4 Hz, 2H, 2 × Ar-H), 6.88 (d, J = 15.2 Hz, 1H, CH = CH), 4.81 (s, 2H, $phCH_2$), 3.88 (d, J = 24.0 Hz, 2H, $phCH_2$), 2.94–2.92 (m, 2H, NCH_2). ^{13}C NMR (100 MHz, $CDCl_3$) δ 164.7, 141.5, 131.6, 131.5, 129.7 (2C), 129.6 (2C), 128.3, 126.7, 117.3, 116.0 (2C), 115.8 (2C), 44.8, 43.6, 29.7. HR-ESI-MS: Calcd. for $C_{18}H_{16}FNO$ $[M + H]^+$: 282.1289, found: 282.1296.

*4.1.1.11. 1-(3,4-dihydroisoquinolin-2(1H)-yl)-3-phenylpropan-1-one (**4 k**).* Yellow oil, 60.8% yield, 97.5% HPLC purity. ^{1}H NMR (400 MHz, $CDCl_3$) δ 8.14 (d, J = 7.6 Hz, 1H, Ar-H), 7.50 (t, J = 7.2 Hz, 1H, Ar-H), 7.38 (t, J = 7.6 Hz, 1H, Ar-H), 7.27–7.24 (m, 5H, 5 × Ar-H), 7.19–7.17 (m, 1H, Ar-H). ^{13}C NMR (100 MHz, $CDCl_3$) δ 176.1, 165.7, 141.1, 140.2, 133.4, 129.6, 129.1, 128.6 (2C), 128.4 (2C), 127.4, 127.3, 126.0, 42.0, 41.0, 31.2, 28.2. HR-ESI-MS: Calcd. for $C_{18}H_{19}NO$ $[M + H]^+$: 266.1539, found: 266.1544.

*4.1.1.12. 1-(3,4-dihydroisoquinolin-2(1H)-yl)-3-(4-hydroxyphenyl) propan-1-one (**4 l**).* Yellow oil, 78.3% yield, 97.8% HPLC purity. ^{1}H NMR (400 MHz, $CDCl_3$) δ 7.19–7.10 (m, 4H, 4 × Ar-H), 7.04–7.01 (m, 2H, 2 × Ar-H), 6.77 (t, J = 8.4 Hz, 2H, 2 × Ar-H), 4.72 (s, 2H, $phCH_2$), 3.57 (t, J = 6.0 Hz, 2H, $phCH_2$), 2.93–2.88 (m, 2H, $phCH_2$), 2.84–2.77 (m, 2H, NCH_2), 2.71–2.65 (m, 2H, NCH_2). HR-ESI-MS: Calcd. for $C_{18}H_{19}NO_2$ $[M + H]^+$: 282.1489, found: 282.1499.

*4.1.1.13. 1-(3,4-dihydroisoquinolin-2(1H)-yl)-3-(4-hydroxy-3-methoxyphenyl)propan-1-one (**4 m**).* Yellow oil, 63.8% yield, 97.9% HPLC purity. ^{1}H NMR (400 MHz, $CDCl_3$) δ 7.19–7.09 (m, 4H, 4 × Ar-H), 6.82 (t, J = 8.0 Hz, 1H, Ar-H), 6.72–6.68 (m, 2H, 2 × Ar-H), 4.73 (s, 2H, $phCH_2$), 3.81 (t, J = 6.0 Hz, 2H, $phCH_2$), 3.80 (s, 3H, OCH_3), 3.59 (t, J = 6.0 Hz, 2H, $phCH_2$), 2.96–2.90 (m, 2H, $CONH_2$), 2.71–2.65 (m, 2H, NCH_2). HR-ESI-MS: Calcd. for $C_{19}H_{21}NO_3$ $[M + H]^+$: 312.1594, found: 312.1605.

*4.1.1.14. (3,4-dihydroisoquinolin-2(1H)-yl)(naphthalen-2-yl)methanone (**4n**).* Yellow oil, 88.1% yield, 97.3% HPLC purity. ^{1}H NMR (400 MHz, $CDCl_3$) δ 7.94 (s, 1H, Ar–H), 7.87 (t, J = 9.0 Hz, 3H, 3 × Ar–H), 7.52 (d, J = 4.4 Hz, 3H, 3 × Ar–H), 7.29 – 7.07 (m, 4H, 4 × Ar–H), 4.78 (d, J = 122.7 Hz, 2H, NCH_2), 3.84 (d, J = 147.8 Hz, 2H, NCH_2), 2.93 (d, J = 53.0 Hz, 2H, CH_2). HR-ESI-MS: Calcd. for $C_{20}H_{17}NO$ $[M + H]^+$: 288.1344, found: 288.1352.

*4.1.1.15. (3,4-dihydroisoquinolin-2(1H)-yl)(1-hydroxynaphthalen-2-yl) methanone (**4o**).* Yellow oil, 816% yield, 97.2% HPLC purity. ^{1}H NMR (400 MHz, $CDCl_3$) δ 11.47 (s, 1H, Ar-OH), 8.37 (d, J = 8.1 Hz, 1H, Ar-H), 7.75 (d, J = 8.0 Hz, 1H, Ar-H), 7.53 (m, 1H, Ar-H), 7.48 (t, J = 7.5 Hz, 1H, Ar-H), 7.36 (d, J = 8.7 Hz, 1H, Ar-H), 7.28 (d, J = 8.7 Hz, 1H, Ar-H), 7.16 (td, J = 9.1, 4.9 Hz, 3H, 3 × Ar-H), 7.07 (d, J = 4.8 Hz, 1H, Ar-H), 4.86 (s, 2H, NCH_2), 3.91 (t, J = 5.9 Hz, 2H, NCH_2), 2.99 (t, J = 5.8 Hz, 2H, CH_2). HR-ESI-MS: Calcd. for $C_{20}H_{17}NO_2$ $[M + H]^+$: 304.1332, found: 304.1341.

*4.1.1.16. (3,4-dihydroisoquinolin-2(1H)-yl)(4-hydroxy-3-methoxyphenyl)methanone (**4p**).* Yellow oil, 63.7% yield, 98.1% HPLC purity. ^{1}H NMR (400 MHz, $CDCl_3$) δ 7.19–7.14 (m, 4H, 4 × Ar-H), 7.03 (s, 1H, Ar-H), 6.97 (dd, J_1 = 6.4 Hz, J_2 = 1.6 Hz, 1H, Ar-H), 6.91 (d, J = 8.4 Hz, 1H, Ar-H), 4.78 (s, 2H, $phCH_2$), 3.85 (s, 3H, OCH_3), 3.80–3.78 (m, 2H, $phCH_2$), 2.93–2.91 (m, 2H, NCH_2). HR-ESI-MS: Calcd. for $C_{17}H_{17}NO_3$ $[M + H]^+$: 284.1281, found: 284.1289.

*4.1.1.17. (E)-1-(4-benzylpiperidin-1-yl)-3-phenylprop-2-en-1-one (**5a**).* Yellow oil, 77.5% yield, 97.4% HPLC purity. ^{1}H NMR (400 MHz, $CDCl_3$) δ 7.65 (d, J = 15.2 Hz, 1H, C = CH), 7.52 (d, J = 6.4 Hz, 2H, 2 × Ar-H), 7.39–7.33 (m, 3H, 3 × Ar-H), 7.30 (t, J = 7.6 Hz, 2H, 2 × Ar-H), 7.21 (t, J = 7.6 Hz, 1H, Ar-H), 7.14 (d, J = 7.6 Hz, 2H, 2 × Ar-H), 6.89 (d, J = 15.6 Hz, 1H, C = CH), 4.71 (d, J = 13.2 Hz, 1H, 1/2 $phCH_2$), 4.09 (d, J = 12.8 Hz, 1H, 1/2 $phCH_2$), 3.05 (t, J = 12.8 Hz, 1H, NCH_2), 2.62 (t, J = 12.8 Hz, 1H, NCH_2), 2.56 (t, J = 7.2 Hz, 2H, NCH_2), 1.85–1.78 (m, 1H,

CH), 1.74 (d, $J = 13.6$ Hz, 2H, CH_2), 1.23–1.21 (m, 2H, CH_2). HR-ESI-MS: Calcd. for $C_{21}H_{23}NO$ $[M + H]^+$: 306.1852, found: 306.1859.

*4.1.1.18. (E)-1-(4-benzylpiperidin-1-yl)-3-(4-hydroxyphenyl)prop-2-en-1-one (**5b**).* Yellow oil, 56.5% yield, 98.2% HPLC purity. ^{1}H NMR (400 MHz, $CDCl_3$) δ 7.57 (d, $J = 15.2$ Hz, 1H, CH = CH), 7.35–7.12 (m, 7H, 7 × Ar-H), 6.86 (d, $J = 8.0$ Hz, 2H, 2 × Ar-H), 6.71 (d, $J = 15.2$ Hz, 1H, CH = CH), 4.69 (d, $J = 9.2$ Hz, 1H, 1/2 phCH$_2$), 4.08 (d, $J = 10.8$ Hz, 1H, 1/2 phCH2), 3.04 (t, $J = 11.2$ Hz, 1H, 1/2 NCH$_2$), 2.64 (t, $J = 11.2$ Hz, 1H, 1/2 NCH$_2$), 2.60–2.53 (m, 2H, NCH$_2$), 1.80–1.71 (m, 3H, CH + CH$_2$), 1.26–1.20 (m, 2H, CH$_2$). HR-ESI-MS: Calcd. for $C_{21}H_{23}NO_2$ $[M + H]^+$: 322.1802, found: 322.1815.

*4.1.1.19. (E)-1-(4-benzylpiperidin-1-yl)-3-(4-hydroxy-3-methoxyphenyl) prop-2-en-1-one (**5c**).* Yield 61.3%, 98.2% HPLC purity. ^{1}H NMR (400 MHz, $CDCl_3$) δ 7.58 (d, $J = 15.2$ Hz, 1H, C = CH), 7.29 (t, $J = 6.8$ Hz, 2H, 2 × Ar-H), 7.21 (t, $J = 7.2$ Hz, 1H, Ar-H), 7.14 (dd, $J_1 = 5.8$ Hz, $J_2 = 1.2$ Hz, 2H, 2 × Ar-H), 7.09 (dd, $J_1 = 6.4$ Hz, $J_2 = 1.6$ Hz, 1H, Ar-H), 6.98 (d, $J = 1.6$ Hz, 1H, Ar-H), 6.91 (d, $J = 8.4$ Hz, 1H, Ar-H), 6.73 (d, $J = 15.2$ Hz, 1H, C = CH), 6.16 (s, 1H, OH), 4.71 (d, $J = 11.2$ Hz, 1H, 1/2 phCH$_2$), 4.00 (d, $J = 11.6$ Hz, 1H, 1/2 phCH$_2$), 3.91 (s, 3H, OCH_3), 3.04 (d, $J = 12.0$ Hz, 1H, 1/2 NCH$_2$), 2.61 (d, $J = 12.0$ Hz, 1H, 1/2 NCH$_2$), 2.58–2.53 (m, 2H, NCH$_2$), 1.84–1.77 (m, 1H, CH), 1.76–1.71 (d, $J = 13.2$ Hz, 2H, CH$_2$), 1.22 (d, $J = 13.2$ Hz, 2H, CH$_2$). ^{13}C NMR (100 MHz, $CDCl_3$) 165.9, 147.6, 147.0, 143.1, 140.0, 129.1 (2C), 128.3 (2C), 127.5, 126.1, 121.9, 115.1, 114.3, 110.1, 56.0, 46.3, 43.0, 42.8, 38.3, 32.8, 31.9. HR-ESI-MS: Calcd. for $C_{22}H_{25}NO_3$ $[M + H]^+$: 352.1907, found: 352.1913.

*4.1.1.20. (E)-1-(4-benzylpiperidin-1-yl)-3-(thiophen-2-yl)prop-2-en-1-one (**5d**).* Light yellow oil, 58.2% yield, 98.1% HPLC purity. ^{1}H NMR (400 MHz, $CDCl_3$) δ 7.75 (d, $J = 15.1$ Hz, 1H, C = CH), 7.25 (m, 3H, 3 × Ar–H), 7.17 (dd, $J = 8.9$, 5.5 Hz, 2H, 2 × Ar–H), 7.11 (d, $J = 7.0$ Hz, 2H, 2 × Ar–H), 6.99 (dd, $J = 5.0$, 3.7 Hz, 1H, Ar-H), 6.66 (d, $J = 15.1$ Hz, 1H, C = CH), 4.65 (s, 1H, 1/2 NCH$_2$), 4.00 (d, $J = 9.4$ Hz, 1H, 1/2 NCH$_2$), 2.99 (s, 1H, 1/2 NCH$_2$), 2.53 (d, $J = 5.4$ Hz, 3H, 1/2 NCH$_2$, CH$_2$), 1.76 (m, 1H, CH), 1.70 (d, $J = 13.3$ Hz, 2H, CH$_2$), 1.20 (m, 2H, CH$_2$). ^{13}C NMR (100 MHz, $CDCl_3$) δ 165.0, 140.7, 140.0, 135.2, 130.0, 129.2 (2C), 128.4 (2C), 128.0, 127.0, 126.1, 116.4, 43.0 (3C), 38.4 (3C). HR-ESI-MS: Calcd. for $C_{19}H_{21}NOS$ $[M + H]^+$: 312.1417, found: 312.1425.

*4.1.1.21. (E)-1-(4-benzylpiperidin-1-yl)-3-(naphthalen-2-yl)prop-2-en-1-one(**5e**).* Yellow oil, 60.9% yield, 98.0% HPLC purity. ^{1}H NMR (400 MHz, $CDCl_3$) δ 8.48 (d, $J = 15.1$ Hz, 1H, C = CH), 8.21 (d, $J = 8.1$ Hz, 1H, Ar-H), 7.81 (d, $J = 7.7$ Hz, 2H, 2 × Ar-H), 7.67 (d, $J = 7.1$ Hz, 1H, Ar-H), 7.45 (dt, $J = 15.5$, 8.1 Hz, 3H, 3 × Ar-H), 7.25 (d, $J = 7.4$ Hz, 2H, 2 × Ar-H), 7.19 (d, $J = 7.3$ Hz, 1H, Ar-H), 7.10 (d, $J = 7.2$ Hz, 2H, 2 × Ar-H), 6.92 (d, $J = 15.2$ Hz, 1H, C = CH), 4.73 (d, $J = 12.3$ Hz, 1H, 1/2 NCH$_2$), 4.04 (d, $J = 12.8$ Hz, 1H, 1/2 NCH$_2$), 2.97 (t, $J = 12.5$ Hz, 1H, 1/2 NCH$_2$), 2.59 (t, $J = 12.7$ Hz, 1H, 1/2 NCH$_2$), 2.50 (t, $J = 6.3$ Hz, 2H, CH$_2$), 1.71 (s, 1H, CH), 1.66 (d, $J = 12.6$ Hz, 2H, CH$_2$), 1.24 – 1.13 (m, 2H, CH$_2$). ^{13}C NMR (100 MHz, $CDCl_3$) δ 165.2, 140.0, 139.6, 133.7, 133.2, 131.5, 129.8, 129.2 (2C), 128.7, 128.4 (2C), 126.7, 126.2, 126.1, 125.5, 124.6, 123.8, 120.8, 46.3, 43.0, 42.7, 38.3, 32.9, 31.9. HR-ESI-MS: Calcd. for $C_{25}H_{25}NO$ $[M + H]^+$: 356.2009, found: 356.2014

*4.1.1.22. (E)-1-(4-benzylpiperidin-1-yl)-2-methyl-3-phenylprop-2-en-1-one (**5f**).* Yellow oil, 71.9% yield, 97.6% HPLC purity. ^{1}H NMR (400 MHz, $CDCl_3$) δ 7.38 – 7.22 (m, 8H, 7 × Ar–H, C = CH), 7.20 (d, $J = 7.2$ Hz, 1H, Ar–H), 7.13 (d, $J = 7.4$ Hz, 2H, 2 × Ar–H), 4.58 (s, 1H, 1/2NCH$_2$), 3.91 (d, $J = 59.4$ Hz, 1H, 1/2NCH$_2$), 3.14 – 2.83 (m, 1H, 1/2NCH$_2$), 2.60 (d, $J = 5.6$ Hz, 1H, 1/2NCH$_2$), 2.55 (d, $J = 6.6$ Hz, 2H, CH$_2$), 2.09 (s, 3H, CH_3), 1.84 – 1.75 (m, 1H, CH), 1.70 (d, $J = 10.3$ Hz, 2H, CH$_2$), 1.28 – 1.11 (m, 2H, CH$_2$). HR-ESI-MS: Calcd. for $C_{22}H_{25}NO$ $[M + H]^+$: 320.2009, found: 320.2020.

*4.1.1.23. 1-(4-benzylpiperidin-1-yl)-2-methylprop-2-en-1-one (**5 g**).* Yellow oil, 81.5% yield, 98.1% HPLC purity. ^{1}H NMR (400 MHz, $CDCl_3$) δ 7.24 (t, $J = 7.3$ Hz, 2H, 2 × Ar-H), 7.15 (t, $J = 7.3$ Hz, 1H, Ar-H), 7.10 (d, $J = 7.2$ Hz, 2H, 2 × Ar-H), 5.09 (s, 1H, 1/2 CH$_2$), 4.97 (s, 1H, 1/2 CH$_2$), 4.52 (s, 1H, 1/2 NCH$_2$), 3.90 (s, 1H, 1/2 NCH$_2$), 2.72 (m, 2H, NCH$_2$), 2.50 (d, $J = 7.0$ Hz, 2H, CH$_2$), 1.91 (s, 3H, CH_3), 1.72 (m, 1H, CH), 1.63 (d, $J = 12.4$ Hz, 2H, CH$_2$), 1.10 (d, $J = 7.2$ Hz, 2H, CH$_2$). HR-ESI-MS: Calcd. for $C_{16}H_{21}NO$ $[M + H]^+$: 244.1696, found: 244.1712.

*4.1.1.24. 1-(4-benzylpiperidin-1-yl)-3-phenylprop-2-yn-1-one (**5 h**).* Yellow oil, 79.3% yield, 98.0% HPLC purity. ^{1}H NMR (400 MHz, $CDCl_3$) δ 7.51 (d, $J = 7.1$ Hz, 2H, 2 × Ar-H), 7.31 (m, 5H, 5 × Ar-H), 7.18 (t, $J = 7.0$ Hz, 1H, Ar-H), 7.12 (d, $J = 7.4$ Hz, 2H, 2 × Ar-H), 4.57 (d, $J = 13.3$ Hz, 1H, 1/2 NCH$_2$), 4.41 (d, $J = 13.2$ Hz, 1H, 1/2 NCH$_2$), 3.04 (t, $J = 12.6$ Hz, 1H, 1/2 NCH$_2$), 2.57 (m, 3H, 1/2 NCH$_2$, CH$_2$), 1.74 (dt, $J = 23.1$, 7.7 Hz, 3H, CH, CH$_2$), 1.19 (dd, $J = 25.4$, 12.6 Hz, 2H, CH$_2$). ^{13}C NMR (100 MHz, $CDCl_3$) δ 152.7, 139.6, 132.1 (2C), 129.8, 128.9 (2C), 128.4 (2C), 128.2 (2C), 125.9, 120.5, 90.1, 81.4, 47.3, 42.7, 41.5, 38.0, 32.3, 31.4. HR-ESI-MS: Calcd. for $C_{21}H_{21}NO$ $[M + H]^+$: 304.1696, found: 304.1702.

*4.1.1.25. (E)-1-(4-benzylpiperidin-1-yl)-3-(4-fluorophenyl)prop-2-en-1-one (**5i**).* Yellow oil, 66.7% yield, 98.2% HPLC purity. ^{1}H NMR (400 MHz, $CDCl_3$) δ 7.60 (d, $J = 15.4$ Hz, 1H, Ar-H), 7.46 (dd, $J = 8.4$, 5.5 Hz, 2H, 2 × Ar-H), 7.27 (t, $J = 7.3$ Hz, 2H, 2 × Ar-H), 7.18 (t, $J = 7.3$ Hz, 1H, Ar-H), 7.12 (d, $J = 7.7$ Hz, 2H, 2 × Ar-H), 7.01 (t, $J = 8.6$ Hz, 2H, 2 × Ar-H), 6.82 (d, $J = 15.4$ Hz, 1H, Ar-H), 4.68 (d, $J = 10.1$ Hz, 1H, 1/2 NCH$_2$), 4.05 (d, $J = 10.4$ Hz, 1H, 1/2 NCH$_2$), 3.00 (s, 1H, 1/2 NCH$_2$), 2.55 (m, 3H, 1/2 NCH$_2$, CH$_2$), 1.76 (m, 3H, CH, CH$_2$), 1.19 (d, $J = 11.2$ Hz, 2H, CH$_2$). HR-ESI-MS: Calcd. for $C_{21}H_{22}FNO$ $[M + H]^+$: 324.1758, found: 324.1765.

*4.1.1.26. 1-(4-benzylpiperidin-1-yl)-3-phenylpropan-1-one (**5j**).* Yellow oil, 73.2% yield, 98.0% HPLC purity. ^{1}H NMR (400 MHz, $CDCl_3$) δ 7.22 (t, $J = 7.3$ Hz, 4H, 4 × Ar-H), 7.14 (dd, $J = 16.8$, 7.8 Hz, 4H, 4 × Ar-H), 7.06 (d, $J = 7.4$ Hz, 2H, 2 × Ar-H), 4.57 (d, $J = 13.1$ Hz, 1H, 1/2 NCH$_2$), 3.62 (d, $J = 13.3$ Hz, 1H, 1/2 NCH$_2$), 2.93 (dd, $J = 11.1$, 4.8 Hz, 2H, NCH$_2$), 2.73 (dd, $J = 18.7$, 7.0 Hz, 1H, 1/2 CH$_2$), 2.52 (dt, $J = 12.8$, 6.3 Hz, 2H, CH$_2$), 2.40 (m, 3H, 3/2 NCH$_2$), 1.63 (m, 1H, CH), 1.55 (m, 1H, 1/2 CH$_2$), 1.49 (d, $J = 12.9$ Hz, 1H, 1/2 CH$_2$), 1.03 (qd, $J = 12.5$, 3.9 Hz, 1H, 1/2 CH$_2$), 0.86 (qd, $J = 12.6$, 3.7 Hz, 1H, 1/2 CH$_2$). ^{13}C NMR (100 MHz, $CDCl_3$) δ 170.6, 141.6, 140.1, 129.2 (2C), 128.6 (2C), 128.6 (2C), 128.4 (2C), 126.2, 126.2, 46.0, 43.1, 42.2, 38.3, 35.3, 32.6, 31.9, 31.8. HR-ESI-MS: Calcd. for $C_{21}H_{25}NO$ $[M + H]^+$: 308.2009, found: 308.2015.

*4.1.1.27. 1-(4-benzylpiperidin-1-yl)-3-(4-hydroxyphenyl)propan-1-one (**5 k**).* Yellow oil, 68.6% yield, 98.1% HPLC purity. ^{1}H NMR (400 MHz, $CDCl_3$) δ 7.27 (t, $J = 7.2$ Hz, 2H, 2 × Ar-H), 7.18 (t, $J = 7.2$ Hz, 1H, Ar-H), 7.10 (d, $J = 7.2$ Hz, 2H, 2 × Ar-H), 7.00 (d, $J = 8.0$ Hz, 2H, 2 × Ar-H), 6.79 (d, $J = 8.0$ Hz, 2H, 2 × Ar-H), 4.60 (d, $J = 13.2$ Hz, 1H, 1/2 phCH$_2$), 3.73 (d, $J = 13.2$ Hz, 1H, 1/2 phCH$_2$), 2.87–2.79 (m, 2H, phCH2), 2.60–2.54 (m, 2H, NCH$_2$), 2.52–2.42 (m, 2H, NCH$_2$), 1.71–1.55 (m, 3H, CH + CH$_2$), 1.14–1.04 (m, 2H, CH$_2$). HR-ESI-MS: Calcd. for $C_{21}H_{25}NO_2$ $[M + H]^+$: 324.1958, found: 324.1969.

*4.1.1.28. (4-benzylpiperidin-1-yl)-3-(4-hydroxy-3-methoxyphenyl) propan-1-one (**5 l**).* Yellow oil, 70.3% yield, 98.1% HPLC purity. ^{1}H NMR (400 MHz, $CDCl_3$) δ 7.28 (t, $J = 7.6$ Hz, 2H, 2 × Ar-H), 7.19 (t, $J = 7.2$ Hz, 1H, Ar-H), 7.11 (d, $J = 7.2$ Hz, 2H, 2 × Ar-H), 6.83 (d, $J = 8.0$ Hz, 1H, Ar-H), 6.72 (s, 1H, Ar-H), 6.68 (dd, $J_1 = 6.4$ Hz, $J_2 = 1.6$ Hz, 1H, Ar-H), 6.85–5.80 (brs, 1H, OH), 4.62 (d, $J = 13.2$ Hz, 1H, 1/2 phCH$_2$), 3.86 (s, 3H, OCH_3), 3.74 (d, $J = 13.6$ Hz, 1H, 1/2 phCH$_2$), 2.88 (t, $J = 7.2$ Hz, 2H, phCH$_2$), 2.84 (t, $J = 13.2$ Hz, 1H, 1/2 NCH$_2$), 2.60–2.55 (m, 2H, COCH$_2$), 2.53–2.48 (m, 2H, NCH$_2$), 2.47 (t, $J = 13.2$ Hz, 1H, 1/2 NCH$_2$), 1.75–1.70 (m, 1H, CH), 1.66 (d, $J = 14.4$ Hz, 1H, 1/2 CH$_2$), 1.58 (d, $J =$

13.2 Hz, 1H, 1/2 CH_2), 1.45–1.04 (m, 1H, 1/2 CH_2), 0.99–0.88 (m, 1H, 1/2 CH_2). HR-ESI-MS: Calcd. for $C_{22}H_{27}NO_3$ $[M + H]^+$: 354.2064, found: 354.2075.

*4.1.1.29. (4-benzylpiperidin-1-yl)(naphthalen-2-yl)methanone (**5 m**).* Yellow oil, 80.5% yield, 97.9% HPLC purity. ^{1}H NMR (400 MHz, $CDCl_3$) δ 7.87 (s, 1H, Ar–H), 7.80 (t, J = 8.1 Hz, 3H, 3 × Ar–H), 7.46 (d, J = 8.9 Hz, 3H, 3 × Ar–H), 7.25 (t, J = 7.3 Hz, 2H, 2 × Ar–H), 7.16 (t, J = 6.0 Hz, 1H, Ar–H), 7.10 (d, J = 7.3 Hz, 2H, 2 × Ar–H), 4.73 (s, 1H, 1/2NCH_2), 3.72 (s, 1H, 1/2NCH_2), 2.79 (d, J = 74.3 Hz, 2H, NCH_2), 2.51 (s, 2H, CH_2), 1.74 (s, 2H, CH_2), 1.50 (s, 1H, CH), 1.23 (dd, J = 36.0, 15.4 Hz, 2H, CH_2). HR-ESI-MS: Calcd. for $C_{23}H_{23}NO$ $[M + H]^+$: 330.1813, found: 330.1819.

*4.1.1.30. (4-benzylpiperidin-1-yl)(1-hydroxynaphthalen-2-yl)methanone (**5n**).* Yellow oil, 74.4% yield, 98.1% HPLC purity. ^{1}H NMR (400 MHz, $CDCl_3$) δ 11.28 (s, 1H, ph-OH), 8.37 (d, J = 8.1 Hz, 1H, Ar-H), 7.74 (d, J = 7.9 Hz, 1H, Ar-H), 7.51 (m, 2H, 2 × Ar-H), 7.25 (m, 5H, 5 × Ar-H), 7.14 (d, J = 7.1 Hz, 2H, 2 × Ar-H), 4.40 (d, J = 13.3 Hz, 2H, NCH_2), 2.92 (t, J = 12.0 Hz, 2H, NCH_2), 2.58 (d, J = 7.1 Hz, 2H, CH_2), 1.83 (dtd, J = 14.2, 7.2, 3.5 Hz, 1H, CH), 1.75 (d, J = 13.5 Hz, 2H, CH_2), 1.31 (ddd, J = 16.6, 13.1, 4.1 Hz, 2H, CH_2). ^{13}C NMR (100 MHz, $CDCl_3$) δ 172.3, 158.3, 140.0, 135.6, 129.2 (2C), 128.5 (2C), 128.5, 127.4, 126.3, 125.7, 125.7, 124.5, 123.7, 117.6, 109.6, 46.5 (2C), 43.1, 38.4, 32.4 (2C). HR-ESI-MS: Calcd. for $C_{23}H_{23}NO_2$ $[M + H]^+$: 346.1802, found: 346.1807.

*4.1.1.31. benzylpiperidin-1-yl)(4-hydroxy-3-methoxyphenyl)methanone (**5o**).* Yellow oil, 68.5% yield, 98.1% HPLC purity. ^{1}H NMR (400 MHz, $CDCl_3$) δ 7.29–7.25 (m, 2H, 2 × Ar-H), 7.19 (t, J = 7.2 Hz, 1H, Ar-H), 7.14 (d, J = 6.8 Hz, 2H, 2 × Ar-H), 6.97 (s, 1H, Ar-H), 6.86 (s, 2H, 2 × Ar-H), 4.62–4.59 (m, 1H, 1/2 phCH_2), 3.85–3.84 (m, 1H, 1/2 phCH_2), 3.83 (s, 3H, OCH_3), 2.87–2.76 (m, 2H, NCH_2), 2.57–2.54 (m, 2H, NCH_2), 1.81–1.75 (m, 1H, CH), 1.69–1.65 (m, 2H, CH_2), 1.26–1.19 (m, 2H, CH_2). HR-ESI-MS: Calcd. for $C_{20}H_{23}NO_3$ $[M + H]^+$: 326.1751, found: 326.1757.

*4.1.1.32. 1-(4-benzylpiperidin-1-yl)ethan-1-one (**5p**).* Yellow oil, 78.1% yield, 97.5% HPLC purity. ^{1}H NMR (400 MHz, $CDCl_3$) δ 7.24 (t, J = 7.4 Hz, 2H, 2 × Ar-H), 7.16 (d, J = 7.3 Hz, 1H, Ar-H), 7.10 (d, J = 7.3 Hz, 2H, 2 × Ar-H), 4.55 (d, J = 13.1 Hz, 1H, 1/2 NCH_2), 3.70 (d, J = 13.4 Hz, 1H, 1/2 NCH_2), 2.90 (dd, J = 19.1, 6.7 Hz, 1H, 1/2 NCH_2), 2.49 (dt, J = 9.7, 5.0 Hz, 2H, 1/2 NCH_2, 1/2 CH_2), 2.41 (m, 1H, 1/2 CH_2), 2.01 (s, 3H, CH_3), 1.70 (m, 1H, CH), 1.62 (m, 2H, CH_2), 1.09 (m, 2H, CH_2). ^{13}C NMR (100 MHz, $CDCl_3$) δ 168.5, 139.7, 128.9 (2C), 128.1 (2C), 125.9, 46.5, 42.8, 41.6, 37.9, 32.3, 31.5, 21.3. HR-ESI-MS: Calcd. for $C_{14}H_{19}NO$ $[M + H]^+$: 278.1539, found: 278.1547.

4.2. Biological activity

4.2.1. Inhibition of AChE and BuChE

The AChE and BuChE inhibitory capacity were assessed by Ellman assay using *ee*AChE, *hu*AChE, *eq*BuChE and human serum BuChE). All the stock solution of test compounds were prepared in DMSO (2.5 mM) and diluted with potassium phosphate buffer (100 mM, pH 7.40, containing KCl 20.2 mM). Donepezil was used as reference compound. The detailed procedure referenced our previous work [32,33].

4.2.2. The reversibility study of huBuChE inhibition

In order to determine the reversibility of *hu*BuChE inhibition by target derivatives, the best BuChE inhibitor was selected to test the recovery of *hu*BuChE inhibition after dilution with time monitoring. The detailed procedure referenced our previous work [33,34].

4.2.3. Human MAO-A and MAO-B inhibition studies

Recombinant human MAO-A and -B were purchased from Sigma-Aldrich. Rasagiline and Kynuramine were used as the positive compound and MAOs substrate, respectively. The final concentration of Kynuramine was 45 μM for MAO-A and 30 μM for MAO-B. The detailed procedure referenced our previous work [34].

4.2.4. Antioxidant activity assay

The antioxidant activity of target compound was measured by the oxygen radical absorbance capacity fluorescein (ORAC-FL) assay. The detailed procedure referenced our previous work [33,35].

4.2.5. Anti-inflammatory property

In order to evaluate the anti-inflammatory property of cinnamic acid hybrids, compound **4b, 4e** and **5 h** with four different concentration (3.5, 7, 14 and 28 μM) were selected to test the effects on LPS-induced PC12 cell injury using 3-(4,5-dimethylthiazol-2-yl)-2,5-diphenyltetrazolium bromide (MTT) assay. The detailed procedure referenced our previous work [33].

4.2.6. Inhibition of self-induced $A\beta_{1-42}$ aggregation

To study self-induced $A\beta_{1\text{-}42}$ aggregation inhibition, a Thioflavin *T*-based fluorometric assay was performed. The procedure referenced our previous work [33,35].

4.2.7. Molecular modeling studies

Docking was utilized to confirm the potential binding of compound **4e** to *hu*BuChE and *hu*MAO-B. The crystal structures of *hu*BuChE (PDB code: 4tpk) and *hu*MAO-B (PDB code: 2 V60) were retrieved from the Protein Data Bank. The 3D structure of **4e** was generated and optimized by molecular mechanics. The detailed procedure referenced our previous work [33,34].

4.2.8. In vitro blood–brain barrier permeation assay

The parallel artificial membrane permeation assay (PAMPA) was used to evaluate the blood–brain barrier penetration of target compounds. Porcine brain lipid (PBL) was purchased from Avanti Polar Lipids. Commercial drugs were obtained from Sigma and Alfa Aesar. The 96-well UV plate (COSTAR) was from Corning Incorporated. The acceptor microplate and donor microplate (PVDF membrane, pore size 0.45 mm) were both from Millipore. According to our previous work, we can infer that compounds with P_e values above 3.44×10^{-6} cm/s could cross the blood–brain barrier [39].

4.2.9. Effects on $AlCl_3$-induced zebrafish AD model

Based on the above results of MNLC, various concentration ***4e*** groups (0.9, 2.7 and 8.0 μg/mL), untreated group and vehicle group (1% DMSO) were used to treat wild-type zerbrafish at 2dpf (n = 30 per group), and the experiment phenomenon were observed and counted for 3 days until 5 dpf. The detailed procedure referenced our previous work [33,35].

Step-down passive avoidance test. Kunming mice at body weight of 18–22 g (six weeks old, either gender) were supplied by the Center of Experimental Animals of Sichuan Academy of Chinese Medicine Sciences (eligibility certification no. SCXK-Chuan2018-19). Mice were maintained under standard conditions with a 12 h:12 h light–dark cycle at 20–22 °C with a relative humidity of 60–70%. Sterile food and water were provided according to institutional guidelines. Prior to each experiment, mice were fasted overnight and allowed free access to water. The detailed procedure referenced our previous work [33,35].

4.2.10. The stability studies of **4e** in artificial gastrointestinal fluid

The artificial gastrointestinal fluids were prepared on the basis of the standard method described in China Pharmacopoeia. The artificial gastric fluid consisted of HCl (0.045 mol/L) and pepsin (10 g/L), while the artificial intestinal fluid consisted of trypsin (10 g/L) and KH_2PO_4 (6.8 g/L), and the pH was adjusted to 6.8 with 0.1 mol/L NaOH. The blank gastric fluid and blank intestinal fluid was similar as described above without pepsin and trypsin. The compound 4e was dissolved with

methyl alcohol to the final concentration 1 mg/mL. The solution of 4e was added to artificial gastric fluid (incubated for 0, 0.5, 1, 2, 3, 4, 6, and 8 h), artificial intestinal fluid (0, 0.5, 1, 2, 3, 4, 6, and 8 h), and the final concentration of 4e solution was 0.01 mg/mL. A volume of 200 μL fluid was withdrawn at different time points and terminated with 400 μL methyl alcohol. The supernatant was harvested by centrifugation at 13,000 × g for 10 min. And the subsequent supernatant collected was analyzed by HPLC [42].

5. Associated content

5.1. *Supporting Information*

The Table S1 and Table S1, and the representative ^{1}H, ^{13}C NMR and HR-ESI-MS spectra for the synthesized compounds were available in supporting information.

Declaration of Competing Interest

The authors declare that they have no known competing financial interests or personal relationships that could have appeared to influence the work reported in this paper.

Acknowledgments

This work was supported by funding from the Key Scientific Research Project of Colleges and Universities in Henan Province (NO. 20A350006), and the Special Project of Nanyang Normal University (2020STP006, SYKF2020032, 2020ZX015, 2020QN036 and 2020QN045).

Appendix A. Supplementary data

Supplementary data to this article can be found online at https://doi.org/10.1016/j.bioorg.2021.104879.

References

[1] World Alzheimer Report, Attitudes to dementia., Alzheimer's Disease International 2019 (2019) 1–13.
[2] W. Jagust, Imaging the evolution and pathophysiology of Alzheimer disease, Nat. Rev. Neurosci. 19 (11) (2018) 687–700.
[3] R.J. Perrin, A.M. Fagan, D.M. Holtzman, Multimodal techniques for diagnosis and prognosis of Alzheimer's disease, Nature 461 (7266) (2009) 916–922.
[4] J.E. Desmarais, S. Gauthier, Alzheimer disease: clinical use of cholinergic drugs in Alzheimer disease, Nat Rev Neurol. 6 (8) (2010) 418–420.
[5] J. Viña, J. Sanz-Ros, Alzheimer's disease: Only prevention makes sense, Eur. J. Clin. Invest. 48 (10) (2018), e13005.
[6] J. Cummings, G. Lee, T. Mortsdorf, A. Ritter, K. Zhong, Alzheimer's disease drug development pipeline: 2017, Alzheimers Dement (N Y). 3 (3) (2017) 367–384.
[7] R. Khoury, J. Rajamanickam, G.T. Grossberg, An update on the safety of current therapies for Alzheimer's disease: focus on rivastigmine, Ther Adv Drug Saf. 9 (3) (2018) 171–178.
[8] W.K. Summers, A.L. Koehler, G.M. Marsh, K. Tachiki, A. Kling, Long-term hepatotoxicity of tacrine, Lancet 1 (8640) (1989) 729.
[9] T. Wang, X.H. Liu, J. Guan, S. Ge, M.B. Wu, J.P. Lin, L.R. Yang, Advancement of multi-target drug discoveries and promising applications in the field of Alzheimer's disease, Eur. J. Med. Chem. 169 (2019) 200–223.
[10] V.S. Gontijo, F.P.D. Viegas, C.J.C. Ortiz, Silva M. de Freitas, C.M. Damasio, M. C. Rosa, T.G. Campos, D.S. Couto, K.S. Tranches Dias, C. Viegas, Molecular hybridization as a tool in the design of multi-target directed drug candidates for neurodegenerative diseases, Curr. Neuropharmacol. 18 (5) (2020) 348–407.
[11] Silva M de Freitas, K.S.T. Dias, V.S. Gontijo, C.J.C. Ortiz, C. Viegas Jr., Multi-target directed drugs as a modern approach for drug design towards Alzheimer's disease: An update, Curr. Med. Chem. 25 (29) (2018) 3491–3525.
[12] Blaikie L, Kay G, Kong Thoo Lin P. Current and emerging therapeutic targets of alzheimer's disease for the design of multi-target directed ligands. Medchemcomm. 2019, 10(12): 2052-2072.
[13] E. Perry, R. Perry, G. Blessed, B. Tomlinson, Changes in brain cholinesterases in senile dementia of Alzheimer type, Neuropathol. Appl. Neurobiol. 4 (1978) 273–277.
[14] N.H. Greig, T. Utsuki, D.K. Ingram, Y. Wang, G. Pepeu, C. Scali, Q.S. Yu, J. Mamczarz, H.W. Holloway, T. Giordano, Selective butyrylcholinesterase inhibition elevates brain acetylcholine, augments learning and lowers Alzheimer β-amyloid peptide in rodent, PNAS 102 (2005) 17213–17218.
[15] U. Košak, B. Brus, D. Knez, S. Žakelj, J. Trontelj, A. Pišlar, R. Šink, M. Jukič, M. Živin, A. Podkowa, F. Nachon, X. Brazzolotto, J. Stojan, J. Kos, N. Coquelle, K. Sałat, J.P. Colletier, S. Gobec, The magic of crystal structure-based inhibitor optimization: development of a butyrylcholinesterase inhibitor with picomolar affinity and in vivo activity, J. Med. Chem. 61 (1) (2018) 119–139.
[16] Q. Li, H. Yang, Y. Chen, H. Sun, Recent progress in the identification of selective butyrylcholinesterase inhibitors for Alzheimer's disease, Eur. J. Med. Chem. 132 (2017) 294–309.
[17] J. Hardy, D.J. Selkoe, The amyloid hypothesis of Alzheimer's disease: progress and problems on the road to therapeutics, Science 297 (5580) (2002) 353–356.
[18] H. Wood, Sequential amyloid-β and tau accumulation foreshadows cognitive decline, Nat Rev Neurol. 16 (8) (2019) 1290–1296.
[19] N.N. Nalivaeva, A.J. Turner, Targeting amyloid clearance in Alzheimer's disease as a therapeutic strategy, Br. J. Pharmacol. 176 (18) (2019) 3447–3463.
[20] S. Schedin-Weiss, M. Inoue, L. Hromadkova, Y. Teranishi, N.G. Yamamoto, B. Wiehager, N. Bogdanovic, B. Winblad, A. Sandebring-Matton, S. Frykman, L. O. Tjernberg, Monoamine oxidase B is elevated in Alzheimer disease neurons, is associated with gamma-secretase and regulates neuronal amyloid beta-peptide levels, Alzheimers Res Ther. 9 (1) (2017) 57.
[21] https://www.alzforum.org/therapeutics/rasagiline.
[22] X. Zhang, X. He, Q. Chen, J. Lu, S. Rapposelli, R. Pi, A review on the hybrids of hydroxycinnamic acid as multi-target-directed ligands against Alzheimer's disease, Bioorg. Med. Chem. 26 (3) (2018) 543–550.
[23] A.A. Maruf, H. Lip, H. Wong, P.J. O'Brien, Protective effects of ferulic acid and related polyphenols against glyoxal- or methylglyoxal-induced cytotoxicity and oxidative stress in isolated rat hepatocytes, Chem. Biol. Interact. 234 (2015) 96–104.
[24] M.O. Villareal, K. Sasaki, D. Margout, C. Savry, Z. Almaksour, M. Larroque, H. Isoda, Neuroprotective effect of Picholine virgin olive oil and its hydroxycinnamic acids component against beta-amyloid-induced toxicity in SH-SY5Y neurotypic cells, Cytotechnology 68 (6) (2016) 2567–2578.
[25] N. Ruwizhi, B.A. Aderibigbe, Cinnamic acid derivatives and their biological efficacy, Int. J. Mol. Sci. 21 (16) (2020) 5712.
[26] S. Chandra, A. Roy, M. Jana, K. Pahan, Cinnamic acid activates PPARalpha to stimulate Lysosomal biogenesis and lower Amyloid plaque pathology in an Alzheimer's disease mouse model, Neurobiol. Dis. 124 (2019) 379–395.
[27] Q. Liao, Q. Li, Y. Zhao, P. Jiang, Y. Yan, H. Sun, W. Liu, F. Feng, W. Qu, Design, synthesis and biological evaluation of novel carboline-cinnamic acid hybrids as multifunctional agents for treatment of Alzheimer's disease, Bioorg. Chem. 99 (2020), 103844.
[28] J.S. Lan, J.W. Hou, Y. Liu, Y. Ding, Y. Zhang, L. Li, T. Zhang, Design, synthesis and evaluation of novel cinnamic acid derivatives bearing N-benzyl pyridinium moiety as multifunctional cholinesterase inhibitors for Alzheimer's disease, J. Enzyme Inhib. Med. Chem. 32 (1) (2017) 776–788.
[29] K. Takao, K. Toda, T. Saito, Y. Sugita, Synthesis of Amide and Ester Derivatives of Cinnamic Acid and Its Analogs: Evaluation of Their Free Radical Scavenging and Monoamine Oxidase and Cholinesterase Inhibitory Activities, Chem Pharm Bull (Tokyo). 65 (11) (2017) 1020–1027.
[30] T. Li, W. Pan, K. Wang, W. Liu, Q. Ma, Z. Sang, Novel ferulic acid-donepezil hybrids as multifunctional agents for the treatment of Alzheimer's disease with butyrylcholinesterase, amyloid-*β*, antioxidant and neuroprotective properties, Lett Drug Des Discov. 14 (8) (2017) 918–929.
[31] Z. Sang, W. Pan, K. Wang, Q. Ma, L. Yu, Y. Yang, P. Bai, C. Leng, Q. Xu, X. Li, Z. Tan, W. Liu, Design, synthesis and evaluation of novel ferulic acid-*O*-alkylamine derivatives as potential multifunctional agents for the treatment of Alzheimer's disease, Eur. J. Med. Chem. 130 (2017) 379–392.
[32] Z. Sang, K. Wang, X. Han, M. Cao, Z. Tan, W. Liu, Design, synthesis, and evaluation of novel ferulic acid derivatives as multi-target-directed ligands for the treatment of Alzheimer's disease, ACS Chem. Neurosci. 10 (2) (2019) 1008–1024.
[33] Z. Sang, K. Wang, J. Shi, W. Liu, X. Cheng, G. Zhu, Y. Wang, Y. Zhao, Z. Qiao, A. Wu, Z. Tan, The development of advanced structural framework as multi-target-directed ligands for the treatment of Alzheimer's disease, Eur. J. Med. Chem. 192 (2020), 112180.
[34] Z. Sang, K. Wang, P. Zhang, J. Shi, W. Liu, Z. Tan, Design, synthesis, in-silico and biological evaluation of novel chalcone derivatives as multi-function agents for the treatment of Alzheimer's disease, Eur. J. Med. Chem. 180 (2019) 238–252.
[35] Z. Sang, K. Wang, J. Shi, X. Cheng, G. Zhu, R. Wei, Q. Ma, L. Yu, Y. Zhao, Z. Tan, W. Liu, Apigenin-rivastigmine hybrids as multi-target-directed liagnds for the treatment of Alzheimer's disease, Eur. J. Med. Chem. 187 (2020), 111958.
[36] G. Zhang, Y. Liu, L. Xu, C. Sha, H. Zhang, W. Xu, Resveratrol alleviates lipopolysaccharide-induced inflammation in PC-12 cells and in rat model, BMC Biotech. 19 (1) (2019) 10.
[37] Z. Xiao, C. Huang, J. Wu, L. Sun, W. Hao, L.K. Leung, J. Huang, The neuroprotective effects of ipriflavone against H_2O_2 and amyloid beta induced toxicity in human neuroblastoma SH-SY5Y cells, Eur. J. Pharmacol. 721 (1–3) (2013) 286–293.
[38] L. Di, E.H. Kerns, K. Fan, O.J. McConnell, G.T. Carter, High throughput artificial membrane permeability assay for blood-brain barrier, Eur. J. Med. Chem. 38 (2003) 223–232.
[39] Z. Sang, K. Wang, P. Bai, A. Wu, J. Shi, W. Liu, G. Zhu, Y. Wang, Y. Lan, Z. Chen, Y. Zhao, Z. Qiao, C. Wang, Z. Tan, Design, synthesis and biological evaluation of novel O-carbamoyl ferulamide derivatives as multi-target-directed ligands for the treatment of Alzheimer's disease, Eur. J. Med. Chem. 194 (2020), 112265.

[40] http://www.molinspiration.com/cgi-bin/properties.
[41] W. Huang, C. Li, Z. Shen, X. Zhu, B. Xia, C. Li, Development of a zebrafish model for rapid drug screening against Alzheimer's disease, J. Pharm. Pharmacol. 4 (2016) 174–185.
[42] T.T. Wu, Q.Q. Guo, Z.L. Chen, L.L. Wang, Y. Du, R. Chen, Y.H. Mao, S.G. Yang, J. Huang, J.T. Wang, L. Wang, L. Tang, J.Q. Zhang, Design, synthesis and bioevaluation of novel substituted triazines as potential dual PI3K/mTOR inhibitors, Eur. J. Med. Chem. 204 (2020), 112637.